

558210

Sandia National Laboratories
Waste Isolation Pilot Plant

Determination of Corrosion Rates from Iron/Lead Corrosion Experiments to be used for Gas Generation Calculations

Work Carried Out under the Analysis Plan for Determination of Gas Generation Rates from
Iron/Lead Corrosion Experiments, AP 159, Rev. 0

To be included in the AP-159 records package

WIPP:1.4.2.2:TD:QA-L:RECERT: 558209

Information Only

APPROVAL PAGE

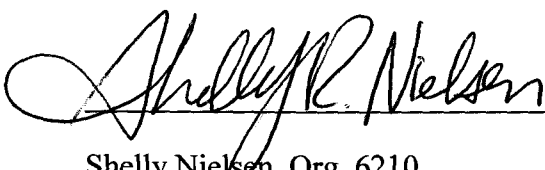
Author:	 _____	<u>9/11/2012</u>
	Gregory T. Roselle, Org. 6212	Date
Technical Reviewer:	 _____	<u>9/11/12</u>
	Je-Hun Jang, Org. 6212	Date
QA Reviewer:	 _____	<u>9-11-12</u>
	Shelly Nielsen, Org. 6210	Date
Management Reviewer:	 _____	<u>9/11/12</u>
	Christi Leigh, Org. 6212	Date

TABLE OF CONTENTS

APPROVAL PAGE	2
TABLE OF CONTENTS	3
LIST OF TABLES	4
LIST OF FIGURES	5
1 Introduction	6
2 Experimental Approach and Methods	9
2.1 Test Coupons	9
2.2 Environmental Conditions	12
2.3 Experimental Brines.....	13
2.4 Experimental Test Matrix	15
3 Experimental Methods	17
3.1 Mixed Flow Gas Control System.....	17
3.2 Coupon Preparation	17
3.3 Sample Loading	18
3.4 Removal and Unloading of Sample Chambers	18
3.5 Determination of Mass Loss and Corrosion Rates	19
4 Results and Discussion	22
4.1 Steel Corrosion Rates.....	22
4.2 Lead Corrosion Rates.....	26
4.3 Application of Results to PA Calculations	30
5 Summary	34
6 References	35
7 Appendix A	38

LIST OF TABLES

Table 1	Composition of ASTM A1008 Low-Carbon Steel	10
Table 2	Composition of Chemical Lead (QQ-L-171e Grade C)	11
Table 3	Composition of GWB and ERDA-6 Brines Used in Steel/Pb Corrosion Studies	13
Table 4	Composition of GWB and ERDA-6 with Organic Ligands for Use in Steel/Pb Corrosion Studies.....	15
Table 5	Experimental Test Matrix	16
Table 6	Chemical Cleaning Procedures by Metal Type	20
Table 7	Average Corrosion Rates ($\mu\text{m}/\text{yr}$) for Steel Samples	24
Table 8	Average Corrosion Rates ($\mu\text{m}/\text{yr}$) for Steel Samples Averaged over all Time Segments	25
Table 9	Average Corrosion Rate ($\mu\text{m}/\text{yr}$) for Lead Samples.....	28
Table 10	Average Corrosion Rates ($\mu\text{m}/\text{yr}$) for Lead Samples Averaged over all Time Segments	29
Table 11	Steel Corrosion PA Parameters from CRA 2009.....	31
Table 12	Revised Steel Corrosion PA Parameter	33
Table A- 1	Summary of Steel Coupon Corrosion Rate Data.....	39
Table A- 2	Summary of Lead Coupon Corrosion Rate Data.....	46

LIST OF FIGURES

Figure 1 Graphical method used to determine coupon mass loss. True mass of the specimen after removal of the corrosion products will be between points B and D.....	21
Figure 2 Average corrosion rates for steel coupons in the various brines plotted as a function of the atmospheric CO ₂ concentration.	25
Figure 3 Average corrosion rates for steel coupons in the various brines plotted as a function of time for each of the atmospheric CO ₂ concentrations.	26
Figure 4 Average corrosion rates for lead coupons in the various brines plotted as a function of the atmospheric CO ₂ concentration.	29
Figure 5 Average corrosion rates for lead coupons in the various brines plotted as a function of time for each of the atmospheric CO ₂ concentrations.	30
Figure 6 Comparison of the cumulative distribution functions (CDF) for the old and new parameter values for CORRMCO ₂	33

1 Introduction

The Waste Isolation Pilot Plant (WIPP) is a deep geologic repository developed by the U.S. Department of Energy (DOE) for the disposal of transuranic (TRU) radioactive waste. The WIPP repository is located within the bedded salts of the Permian Salado Formation, which consists of interbedded halite and anhydrite layers overlaying the Castile Formation. Containment of TRU waste at the WIPP is regulated by the U.S. Environmental Protection Agency (EPA) according to requirements set forth in Title 40 of the Code of Federal Regulations (CFR), Part 191. The DOE demonstrates compliance with containment requirements by means of performance assessment (PA). WIPP PA calculations are used to estimate the probability and consequence of radionuclide releases from the repository to the accessible environment for a regulatory period of 10,000 years after facility closure.

The WIPP PA includes modeling the consequences of future inadvertent human intrusions into the repository by drilling for resources. Such intrusions could lead to a postulated release of radionuclides to the accessible environment before the end of the 10,000 year regulatory period. To accomplish this, the DOE has examined different drilling scenarios, which involve the penetration of the repository by one or more drill holes; some of the scenarios also involve the possibility of the penetration of a pressurized Castile brine reservoir (U.S. DOE, 2009). The estimated quantity of radionuclides released to the accessible environment following penetration of the repository depends on the chemistry of these radioelements. For example, plutonium (Pu) is less soluble when it speciates in lower oxidation states, such as Pu(III) and Pu(IV), than in higher oxidation states, such as Pu(VI). Thus it follows that in order to minimize the release of such radionuclides from the repository it is desirable to maintain all such species in their least-soluble form (i.e., low oxidation states).

The nature of the environment within the WIPP following closure will, to a large extent, control the speciation of the radionuclides within the waste. More specifically, there are components contained within the waste that can impact the oxidative or reductive nature of the environment, such as metals undergoing active corrosion. If metals undergo active corrosion within the WIPP, the corrosion process will serve to maintain electrochemically reducing conditions. The predominant metals within the WIPP will be iron (Fe) in the form of low-carbon

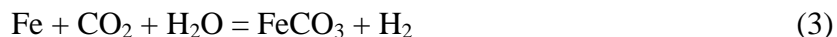
steel and chemical-grade lead (Pb). These metals are present within the waste itself, as well as the containers used to hold the waste during emplacement. The current inventory predicts that 280 and 599 kg/m³ of Fe and Fe-base alloys will be present in the contact handled (CH) and remote handled (RH) wastes, respectively. Also 0.013 and 420 kg/m³ of Pb will be present in the CH and RH wastes, respectively (Crawford 2005). The corrosion behavior of these materials, specifically the kinetics of the corrosion reaction, will be controlled by the availability of water (in brine) at the metal surface, as well as the internal atmosphere within the WIPP. In addition to Fe and Pb, the waste disposed within WIPP contains significant quantities of cellulosic, plastic and rubber (CPR) materials. With time, microbial activity may consume some portion of the CPR materials, resulting in generation of significant quantities of carbon dioxide (CO₂), hydrogen sulfide (H₂S), hydrogen (H₂), nitrogen (N₂) and methane (CH₄).

Steel corrosion and organic-material biodegradation have been identified as major gas-generation processes in the Waste Isolation Pilot Plant (WIPP) repository (Brush, 1995). Gas production will affect room closure and chemistry (Butcher, 1990; Brush, 1990). Wang and Brush (1996) provided estimates of gas-generation parameters for the long-term WIPP performance assessment based on experimental work of Telander and Westerman (1993, 1997). These parameters included steel corrosion rates under inundated and humid conditions, the stoichiometric factors of gas generation reactions, and the probability of the occurrence of organic material biodegradation.

The interaction of steel and lead in the WIPP with repository brines will result in the formation of H₂ gas due to anoxic corrosion of the metals. The rate of H₂ gas generation will depend on the corrosion rate and the type of corrosion products formed. As explained in Brush (1990) two possible anoxic corrosion products of steel in the absence of CO₂ are Fe₃O₄ and (Fe,Mg)(OH)₂ via the reactions:



In the presence of microbially-produced CO₂ steel corrosion can proceed via the reaction:



It is possible that other corrosion products (e.g. green rust, hibbingite, etc.) may also form (Nemer, 2011). For example, if green rust $[\text{Fe(III)}_2\text{Fe(II)}_4(\text{OH})_{12}\text{CO}_3 \cdot 2\text{H}_2\text{O}]$ were identified as the major corrosion product then the corrosion reaction would be written as:



The identification of the corrosion products allows the stoichiometric factors of gas generation reactions to be determined. The anoxic corrosion of Pb could also result in H_2 gas generation via the formation of PbO in the CO_2 -free environments and PbCO_3 in the presence of CO_2 :



Since the analysis of Wang and Brush (1996), a new series of steel and lead corrosion experiments has been conducted under Test Plan TP 06-02, *Iron and Lead Corrosion in WIPP-Relevant Conditions* (Wall and Enos, 2006). The object of these experiments has been to determine steel and lead corrosion rates under WIPP-relevant conditions. Telander and Westerman (1993, 1997) measured H_2 generation rates directly and from those measurements were then able to calculate metal corrosion rates. However, the current experiments under Test Plan 06-02 directly measured metal corrosion rates. The purpose of this analysis report is to describe the calculations needed to determine new corrosion rates for steel and lead in the WIPP performance assessment. It is important to note that the current WIPP PA model does not consider gas generation due to the corrosion of lead. However, the possible use of shielded containers in the WIPP will significantly increase the amount of Pb in the repository (Dunagan et al., 2007). Thus, Pb corrosion rates were also determined in this study.

The work presented in this analysis report was conducted under Test Plan TP 06-02, *Iron and Lead Corrosion in WIPP-Relevant Conditions* (Wall and Enos, 2006) and documents the results for Tasks 1, 3 and 4 of Analysis Plan AP-159, *Analysis Plan for Determination of Gas Generation Rates from Iron/Lead Corrosion Experiments* (Roselle, 2012).

2 Experimental Approach and Methods

The purpose of these experiments was to assess the corrosion behavior of carbon steel and Pb used to contain CH and RH waste under WIPP-relevant conditions. Specifically, the experiments aim to determine the corrosion rates of these metals and the nature of the corrosion products that will form. The environmental conditions and samples used for this set of experiments are set up to be representative of the conditions that are expected in the WIPP following its closure. During these experiments steel and lead coupons were immersed in different WIPP-relevant brines or hung in WIPP-relevant atmospheric conditions for a period of two years. A subset of samples was removed from the experiments for analysis at six month intervals. The following subsections describe the types of metal coupons used and the environmental conditions employed in the experiments.

2.1 Test Coupons

In general, four different container forms are used to dispose of CH waste within the WIPP: drums (55, 85 and 100 gallons in size), standard waste boxes, ten drum overpacks and standard large boxes. These containers are constructed using a range of different carbon and high-strength, low alloy (HSLA) steels. Wall and Enos (2006) have shown that the majority of the steel present in the WIPP (from waste containers) will be of a composition defined either by ASTM A36, ASTM A1008 or ASTM A1011 with by far the largest quantity (approximately 94%) being defined by ASTM A1008, which is used for waste drums. The steels specified in A1008 and A1011 are similar with the exception of the method of production. A1008 is cold-rolled whereas A1011 is hot-rolled. While this will yield different mechanical properties, it has been shown by Telander and Westerman (1993, 1997) that the two will behave similarly in WIPP-relevant brine corrosion tests. ASTM A36 steels differ in composition from the other two in that they have higher C, Mn and Si contents, although A36 steels are still classified as low carbon steels. While it would be interesting to study the effects of brine corrosion over the entire range of steel compositions present in the WIPP, the number of coupons required would be prohibitive. Therefore, only one steel composition (ASTM A1008) was chosen for evaluation in this study. It should be noted that the use of only ASTM A1008 steel is a deviation from the test plan (TP 06-02), which calls for ASTM A36 to be used as well.

The ASTM A1008 steel coupons were obtained from a commercial vendor (Alabama Specialty Products, Inc., Munford, AL) under the Nuclear Waste Management Procedure NP 4-1. The certified composition of the steel coupons is given in Table 1. The coupons are 2 x 1.5 x 1/16 inches with a 3/16 inch diameter hole centered 0.25 inches from the end of the coupon. The coupon surfaces have been finished to 120 grit.

Table 1 Composition of ASTM A1008 Low-Carbon Steel

Element	Weight Percent
Al	0.026
C	0.050
Ca	0.001
Cr	0.040
Cu	0.110
Fe	balance
Mn	0.250
Mo	0.010
N	0.009
Nb	0.003
Ni	0.040
P	0.006
S	0.005
Si	0.010
Sn	0.007
Ti	0.002
V	0.002

Source: Material Test Report for AE960
(ERMS 551552)

The estimated quantity of Pb present in the repository from both the waste and its containers is 3.0×10^6 kg (Wall and Enos, 2006, Section 7.5.2). The vast majority of this Pb is contained in the lids of the packaging and not in the waste itself. Additionally, the DOE has been approved to use shielded (Pb-lined) containers in the WIPP, which will dramatically increase the mass of Pb emplaced in the WIPP. If implemented, the use of shielded containers could increase the mass of Pb by nearly ten-fold to 2.7×10^7 kg (Dunagan et al., 2007). The drawings for neither the current RH containers (Hertelendy, 1984) nor the proposed shielded containers (Sellmer, 2007) specify the Pb alloy to be used. Several specifications exist for Pb alloys. This includes the military specification QQ-L-171e, which in turn calls ASTM B29. This alloy is defined as chemical-copper lead and is nominally 99.9% Pb. The specific Pb alloy chosen for this study is the military specification Grade C, which is specified for chemical use. Lead coupons were obtained from Medi-Ray, Inc. (Tuckahoe, NY) also under NP 4-1. The certified composition of the lead coupons is given in Table 2. Lead coupon dimensions and surface finishing are the same as for the steel coupons.

Table 2 Composition of Chemical Lead (QQ-L-171e Grade C)

Element	Weight Percent
Ag	0.010
Bi	0.015
Cd	0.001
Cu	0.070
Fe	0.001
Ni	0.001
Pb	99.900
Sb+Sn+As	0.001
Zn	0.001

Source: Certificate Of Compliance and Inspection
Metal Coupon, Lot 32829 (ERMS 551551)

2.2 Environmental Conditions

The environmental conditions used for this set of experiments are set up to be representative of the conditions that are expected in the WIPP following closure. These conditions include temperature, relative humidity, atmosphere and sample positioning.

The post-closure temperature within the waste disposal panels at WIPP is assumed to be 28°C. This is based on in-situ temperature measurements made within WIPP Room H (Munson et al., 1987). However, in the Fe/Pb corrosion experiments a temperature of 26°C is used because it is easier to control the relative humidity within the experiments at 26°C instead of 28°C. It is assumed that a 2°C reduction in the experimental temperature will have no effect on the corrosion rates in the experiments. Note that this is a deviation from the test plan, TP 06-02.

Brush (2005) conducted a series of FMT calculations for each of the brines expected in the WIPP. Those calculations show that the equilibrium relative humidity present in the headspace over each of these brines is effectively equivalent at 72%. Based on these calculations, the relative humidity in the Fe/Pb corrosion experiments will be maintained at 72% ±10%.

As stated previously the predicted atmosphere within the WIPP will be anoxic due to the consumption of O₂ by corrosion of metals within the WIPP. In addition, the microbial consumption of the CPR materials in the waste will produce a combination of inert (e.g. N₂ and CH₄) and reactive (e.g. CO₂ and H₂S) gases. In the Fe/Pb corrosion experiments N₂ is substituted for CH₄ as the inert carrier gas to ease Environmental Safety and Health (ES&H) concerns. Although the test plan (TP 06-02) covering these experiments calls for the use of H₂S, no experiments are being conducted at this time with H₂S due to ES&H concerns. Four different atmospheric compositions are being used in these experiments to investigate the effect of CO₂ concentration on the corrosion rates. The four atmospheres are 0 ppm CO₂ (100% N₂), 350 ppm CO₂, 1500 ppm CO₂ and 3500 ppm CO₂. The O₂ concentration in each of the experimental lines is maintained to values less than 5 ppm.

Due to the limited quantity of brine that is predicted to permeate into the waste, it is reasonable to assume that not all of the material will come into contact with liquid brine. Thus, the two coupon types described in Section 2.1 will be evaluated while fully inundated by the

brine, partially submersed in the brine and while exposed only to the humid atmosphere above the brine.

2.3 Experimental Brines

Two brines are predicted to come into contact with the waste over time. These brines are referred to as ERDA-6 and GWB. Both of these brines are synthetic in that they represent an average composition based on numerous brines collected from the field. ERDA-6 is representative of brines present in the Castile Formation, whereas GWB represents Salado Formation brines. Once either of these brines is introduced into the WIPP they will equilibrate with the engineered barrier (MgO) and the host rock (primarily halite and anhydrite). The compositions of GWB and ERDA-6 equilibrated with periclase (MgO), halite and anhydrite are given in the results of FMT calculations completed for the CRA 2005 PABC. The brines used in the Fe/Pb corrosion experiments were synthesized based on the predicted composition from FMT Runs 8 (GWB) and 12 (ERDA-6) (see Table 4 in Brush, 2005). The composition of the brines formulated for use in the experiments is given in Table 3.

Table 3 Composition of GWB and ERDA-6 Brines Used in Steel/Pb Corrosion Studies

Chemical Species	GWB	ERDA-6
	Concentration (molal)	Concentration (molal)
Na ⁺	4.98	6.05
K ⁺	0.559	0.109
Li ⁺	5.05×10 ⁻³	---
Ca ²⁺	1.24×10 ⁻²	1.28×10 ⁻²
Mg ²⁺	0.635	0.121
Cl ⁻	6.30	6.00
Br ⁻	3.18×10 ⁻²	1.24×10 ⁻²
SO ₄ ²⁻	0.209	0.191
B ₄ O ₇ ²⁻	4.73×10 ⁻²	1.77×10 ⁻²

Source: WIPP-FePb-3 p. 51 (ERMS 550783)

The WIPP waste will contain significant amounts of acetate, citrate, EDTA and oxalate at closure time. Brush and Xiong (2005) calculated the concentration of these ligands for the CRA 2005 PABC. These ligands are important to consider for the WIPP PA, as they influence the solubility of actinides in the WIPP. Additionally, there are indications in the literature that all of these organic ligands can have a significant impact on the electrochemical behavior of both Fe and Pb (e.g., Saltykov et al., 1989; Sankarapavinasam et al., 1989a, 1989b; Kubal and Panacek, 1995; Pletcher et al., 2005). While none of these studies have evaluated the impact that low concentrations will have in WIPP relevant brines, they strongly suggest that the organic ligands may have an impact on the corrosion process.

Thus, the Fe/Pb corrosion experiments were also done in GWB and ERDA-6 with organic ligand concentrations equal to those given in Brush and Xiong (2005) except for the oxalate species. The oxalate concentration given in Brush and Xiong (2005) was determined by taking the total mass of oxalate present in the waste and dividing by the minimum brine volume necessary for a release in the PA calculations. However, this value is above the solubility limit for oxalate, as predicted by the FMT calculations. Therefore, the oxalate concentration used in the Fe/Pb corrosion experiments was set equal to the predicted concentration in ERDA-6, which is lower than that predicted for GWB. Table 4 lists the concentrations of the brines synthesized with organic ligands that are used in this study. The major element compositions are slightly different from those in Table 3 because of the addition of the organic salts needed to synthesize these brines.

Test plan, TP 06-02 calls for the use of eight different brines in the Fe/Pb corrosion experiments. These eight brines include the four described above as well as the same brines without equilibration with MgO. In order to reduce the number of experiments to a more manageable number it was decided to only use those four brines that were equilibrated with MgO, which is a deviation from the original matrix in the test plan.

Table 4 Composition of GWB and ERDA-6 with Organic Ligands for Use in Steel/Pb Corrosion Studies

Chemical Species	GWB Concentration (molal)	ERDA-6 Concentration (molal)
Na ⁺	4.99	5.96
K ⁺	0.563	0.109
Li ⁺	5.05×10 ⁻³	---
Ca ²⁺	1.03×10 ⁻²	1.22×10 ⁻²
Mg ²⁺	0.663	0.179
Cl ⁻	6.24	5.98
Br ⁻	3.19×10 ⁻²	1.24×10 ⁻²
SO ₄ ²⁻	0.262	0.203
B ₄ O ₇ ²⁻	4.76×10 ⁻²	1.77×10 ⁻²
EDTA	8.85×10 ⁻⁶	9.99×10 ⁻⁶
Oxalate	3.38×10 ⁻⁴	3.35×10 ⁻⁴
Citrate	9.09×10 ⁻⁴	9.04×10 ⁻⁴
Acetate	1.19×10 ⁻²	1.19×10 ⁻²

Source: WIPP-FePb-3 p. 52 (ERMS 550783)

2.4 Experimental Test Matrix

The entire range of experimental variables is summarized in Table 5. This combination of experimental conditions, material types and time segments results in 288 unique experiments. In addition, three replicate coupons are used for each of the experimental conditions resulting in a total of 864 coupons (432 for lead and 432 for steel).

Also shown in Table 5 are the matrix identifiers used in formulating unique sample numbers. The naming convention used follows this format: Aa-Bb-#### - X – Yz, where Aa is the material type, Bb the brine (or “Atm” for humid samples), #### the atmosphere, X the time segment, Y the replicate number (1 to 3) and z the sample position (left blank for humid position). Thus, sample number Fe-Go-1500-6-1f indicates the first replicate of a steel coupon fully inundated in GWB organic brine in a 1500 ppm CO₂ atmosphere for six months.

Table 5 Experimental Test Matrix

Condition	Variable	Matrix Identifier
Material Type	ASTM A1008 Steel	Fe
	QQ-L-171e Grade C Lead	Pb
Brine	GWB	G
	GWB with organics	Go
	ERDA-6	E
	ERDA-6 with organics	Eo
Sample Positioning	Fully Inundated	f
	Partially Submerged	p
	Humid Atmosphere	Atm
Atmosphere	0 ppm CO ₂ (balance N ₂)	0000
	350 ppm CO ₂ (balance N ₂)	0350
	1500 ppm CO ₂ (balance N ₂)	1500
	3500 ppm CO ₂ (balance N ₂)	3500
Time Segment	6 months	6
	12 months	12
	18 months	18
	24 months	24
Fixed Properties (constant for all experiments)	Temperature – 26 °C	--
	Relative Humidity – 75% ± 10%	--
	O ₂ concentration < 5 ppm	--
Note: [2 Material types × 4 Brines × 2 Positions (wet) × 4 Atmospheres × 4 Time segments] +		
[2 Material type × 1 Position (humid) × 4 Atmospheres × 4 Time segments] = 288 experiments		

3 Experimental Methods

3.1 Mixed Flow Gas Control System

Previous corrosion experiments (e.g., Telander and Westerman, 1993; 1997) have been conducted in closed systems in which the atmosphere in the experiments changes as a function of corrosion. This method uses measurements of the head gas composition to estimate the amount and type of corrosion occurring in the experiments. However, such experiments result in head space gas compositions that change over time and may not reflect the expected conditions in the WIPP after closure. Therefore, the current Fe/Pb corrosion experiments are being conducted in a continuous flow setup that allows the atmospheric composition to be fixed at constant values. A specially-built gas flow system known as the Mixed Flow Gas Control System (MFGCS) is being used to house the experiments. The MFGCS is a continuous flow system designed to create and maintain a controlled environment for the Fe/Pb corrosion experiments. The variables controlled by the MFGCS include the oxygen level, humidity level and N₂/CO₂ gas concentrations. The system is continuously monitored real time by a data acquisition system (DAS) to continuously assess various experimental and operational parameters. The specific details of the MFGCS can be found in the six month experimental report (Roselle, 2009) and the MFGCS System Pressure Safety Package (Schuhen, 2007).

3.2 Coupon Preparation

Prior to emplacement in the experiments each coupon was measured, cleaned and pre-weighed. All measurements were recorded in the appropriate scientific notebook. Coupons were measured to an accuracy of ± 0.025 mm. For each coupon three measurements of the width, length and thickness were made. The averages of these three measurements were then used to calculate the surface area for each coupon (see Appendix A). The pre-cleaning processes used for the steel and lead coupons were based on recommendations in ASTM G1-03 (ASTM, 2003). Steel coupons were cleaned by degreasing with a commercially available TSP (trisodium phosphate) substitute followed by rinsing with de-ionized (DI) water. Coupons were then rinsed with ethanol and allowed to air dry. Lead coupons were cleaned by degreasing with the TSP

substitute solution and then immersed in a solution of boiling 1% acetic acid for two minutes. After boiling, the coupons were submerged in a beaker of DI water until all coupons had been cleaned in the acid solution. The beaker containing the submerged coupons was then placed into an anoxic glovebox. The lead coupons were then removed from the DI water and allowed to air dry under anoxic conditions. This step was necessary because air drying in the laboratory produced immediate oxidation of the lead coupons. Once the coupons were dry they could then be removed from the glovebox for further preparation. After cleaning, the mass of all coupons was determined to an accuracy of 0.0001 grams. Coupons were then photographed front and back. All coupons were stored inside a desiccator in the anoxic glovebox until loaded in a sample test chamber.

3.3 Sample Loading

After the preparation steps outlined in Section 3.2, the coupons are ready to be placed into the sample test chambers described in Roselle (2009). The sample test chambers are placed into the anoxic glovebox with the coupons and all loading/unloading operations are done inside the glove box. There are eight sample chambers used for each of the four experimental gas streams (e.g. 0 ppm CO₂, 350 ppm CO₂, etc.): four chambers for Pb coupons (one for each of the four time segments) and four for steel coupons. Each test chamber includes eight HDPE containers for the brines (four for fully immersed and four for partially submerged coupons). The three replicate coupons for each setup are separated by nylon spacers and attached to an acrylic hanger with a nylon machine bolt. Each set of replicate coupons is placed into the same brine container. The brine containers are filled with approximately 120 mL of the appropriate brine for the fully immersed replicates and 75 mL of brine for the partially submerged replicate sets. The humid atmosphere set of replicates are hung from the top of the chamber at the end of the brine buckets. Once the chamber has been loaded the end cap is sealed into place and the chamber is removed from the glove box and attached to the MFGCS.

3.4 Removal and Unloading of Sample Chambers

At the conclusion of the experiment a sample chamber is disconnected from the MFGCS and placed into the anoxic glove box. Once the chamber is in the glove box its end cap is

removed and the brine containers with the coupon hangers are taken out of the sample test chamber. The coupon replicate set is then removed from the brine and given a light rinse with DI water to remove any residual brine on the coupons. The hanger with the replicate coupons is then set aside and allowed to air dry inside the glove box for several hours. Once the coupons are removed from the brine container the pH of the brine is measured. The brine is then poured in a glass serum bottle and the bottle is sealed and crimped. All brine bottles are stored in the glove box for later chemical analysis.

After the replicate coupon sets have dried the three coupons are removed from the hangers. Two of the three replicates will be used to determine the weight loss during the experiments. The process used to determine weight loss is discussed below. The third replicate coupon is used for characterizing the corrosion products that formed (also discussed below). Each coupon is photographed prior to being cleaned for the weight loss measurements or material characterization activities. Coupons are stored inside the glove box until needed for analysis.

3.5 Determination of Mass Loss and Corrosion Rates

After the corrosion tests have been completed, two of the three replicate coupons for each test condition were chemically cleaned in order to remove all of the corrosion products. The mass of the coupons after cleaning is compared to the initial mass and the difference represents the loss of material to corrosion. The mass loss can then be used to calculate a corrosion rate.

There are numerous standard procedures that outline requirements for the cleaning of corrosion samples: ISO 8407:1991, NACE Standard TM0169-2000 and ASTM G 1 – 03. For the most part, each of these standard procedures outlines nearly identical requirements and all coupons were cleaned per the requirements outlined in these standards. Where there are differences between the standards, the source for a particular requirement that was used will be noted. The cleaning process included multiple cycles of chemical etching, brushing with a nonmetallic soft bristle brush followed by rinsing with deionized water. Following each cleaning cycle the coupons were dried and weighed with the weight for each cycle being recorded in the scientific notebook. A minimum of five cleaning cycles was performed for each coupon. The details of the chemical cleaning solutions used for each material type are shown in Table 6.

Table 6 Chemical Cleaning Procedures by Metal Type

Material	Chemical	Time	Temperature	Source ¹
Iron (Fe)	concentrated HCl + 50 g/L SnCl ₂ + 20 g/L SbCl ₃	25 min max.	Cold	A
	500 mL conc. hydrochloric acid (HCl) 3.5 g hexamethylene tetramine Reagent water to make 1000 mL	10 min	20 to 25 °C	B
Lead (Pb)	250 g ammonium acetate (CH ₃ COONH ₄) Reagent water to make 1000 mL	5 min	60 to 70 °C	B

¹Source: A, NACE Standard TM0169-2000; B, ASTM G 1 – 03.

Because the above cleaning procedures remove some amount of base metal in addition to the corrosion products a procedure needs to be employed that corrects the weight loss measurements for the base metal loss. This study uses a procedure of graphical analysis based on multiple cleaning cycles in order to extrapolate the actual weight loss due to corrosion from the total measured weight loss. The graphical analysis method is outlined in ISO 8407:1991 and is shown schematically in Figure 1. The mass of a coupon should have a linear relationship with respect to the cleaning cycles as long as the duration of each cycle is the same. A plot of the mass versus cleaning cycles ideally results in two lines (AB and BC in Figure 1). Line AB characterizes the removal of corrosion products and minor amounts of base metal, whereas line BC is the result of removal of the base metal substrate after all corrosion products have been removed. Extrapolation of line BC to the 0th cleaning cycle (point D) provides the true mass of the coupon without the corrosion products on the surface at zero cleaning cycles. For the purposes of determining mass loss in this study, point D is taken as the final weight.

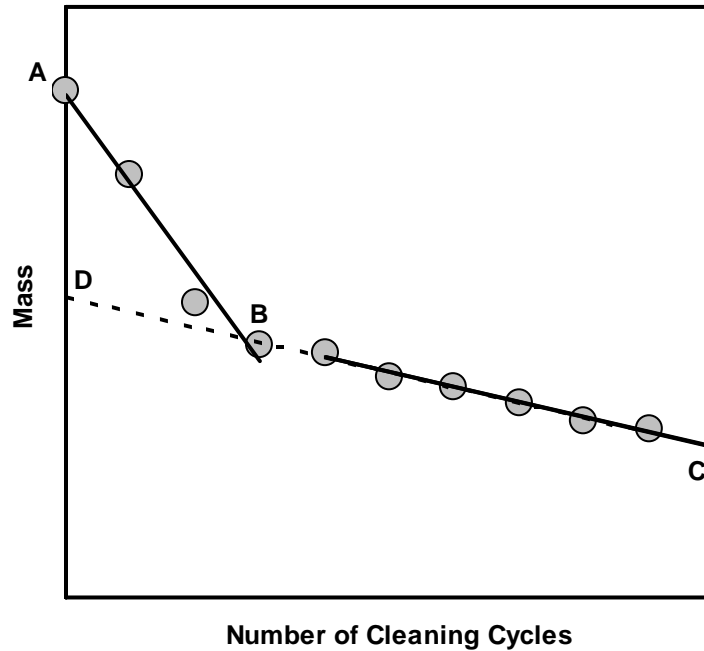


Figure 1 Graphical method used to determine coupon mass loss. True mass of the specimen after removal of the corrosion products will be between points B and D.

The raw cleaning cycle data and graphical analysis results for each coupon are given in appendices of Roselle (2009, 2010, 2011a, 2011b). Corrosion rates are calculated from the mass loss data according to the following formula (NACE, 2000):

$$rate = \frac{W \times 87.6}{SA \times t \times \rho} \times 1000 \quad (7)$$

where *rate* is the corrosion rate in $\mu\text{m}/\text{yr}$, *W* the mass loss (mg), *SA* the exposed surface area of the coupon (cm^2), *t* the exposure duration (hours), ρ the metal density (g/cm^3) and 1,000 converts the rate from mm/yr to $\mu\text{m}/\text{yr}$. Metal densities of $7.872 \text{ g}/\text{cm}^3$ and $11.340 \text{ g}/\text{cm}^3$ were used for steel and lead, respectively (MatWeb, 2009).

4 Results and Discussion

There are four tasks associated with AP-159. The current analysis report discusses results for three of these tasks. Task 1 involves the calculation of mass loss data and the resulting corrosion rates for each of the relevant experimental coupons. Sections 4.1 and 4.2 summarize the corrosion rates determined for this task. Detailed discussions of the weight loss data and corrosion rates are presented in Roselle (2009, 2010, 2011a, 2011b). The determination of the corrosion products is the subject of Task 2 and is not covered in this analysis report. Preliminary observations, however, can be found in Roselle (2009, 2010, 2011a, 2011b). Task 3 was to calculate gas generation rates based on the corrosion rates determined in Task 1. This task will not be completed because the data are not needed for the performance assessment calculations. The gas generation rates are calculated directly within the PA model code BRAGFLO. Section 4.3 outlines the development of revised input parameters for the PA model, which satisfies Task 4 of AP-159.

4.1 Steel Corrosion Rates

Table 7 gives the steel coupon average corrosion rates calculated from the weight-loss and surface area measurements for each brine type and the humid samples as a function of CO₂ concentration and experimental duration. The average corrosion rates for the different brine types are calculated using the results for both the fully immersed and partially submerged coupons for each brine type. In Table 8 corrosion rates are given that have been averaged over all of the time segments for each brine type and CO₂ concentration.

The average steel corrosion rates presented in Table 8 are plotted as a function of CO₂ concentration in Figure 2. A number of important observations can be made from this plot. First, it can be seen that samples hung only in the humid atmosphere essentially exhibit no corrosion regardless of the CO₂ concentration. This is consistent with the appearance of the coupons at the conclusion of the experiments. As documented in Roselle (2009) the humid coupons have the same shiny appearance at the conclusion of the experiments as they did when initially placed into the experimental chambers. A second observation from Figure 2 is that there is a strong correlation between corrosion rates and CO₂ concentration for all brine types. In

general, corrosion rates increase as a function of increasing CO₂ concentrations. Finally, it can be seen that there are differences in the corrosion rates between the different brine types. The ERDA-6 brines appear to be more corrosive than the GWB brines by a factor of more than 3 at the highest CO₂ concentration. It also appears that the addition of organic ligands to the ERDA-6 brine results in significantly less corrosion than the organic free ERDA-6. This does not appear to be the case for GWB. From Figure 2 it can be seen that there is little to no difference in the corrosion rates for the two GWB brine types.

In Figure 3 the corrosion rates presented in Table 7 are plotted as a function of time for each CO₂ concentration and brine type. In these plots it can be seen that in general the corrosion rates for each CO₂ concentration remain relatively constant beyond the first 200 days (approx. 6 months) of experimental duration. There are, however, a couple of exceptions to this observation. First, the corrosion rates in the 3500 ppm experiments may be showing a slight decrease with time, which may be an indication of passivation of the coupon surfaces. Second, the ERDA-6 samples for the 0 and 350 ppm experiments show a spike in corrosion rates at approximately 800 days (24 months). These experiments exhibited other anomalies at the time of their termination such as pH measurements and total Fe concentrations that were outliers from the other samples (as documented in scientific notebooks WIPP-FePb-4). In addition, these experiments experienced significant dehydration during their 24 month duration and water was added to the brine containers (see WIPP-FePb-3 Supplemental Binder C). For these reasons it is likely that the corrosion rates determined from these experiments are suspect. However, they are included in the averages because there is not strong enough evidence to exclude them.

Table 7 Average Corrosion Rates ($\mu\text{m}/\text{yr}$) for Steel Samples

Brine	Exposure Duration (months)			
	6	12	18	24
0 ppm CO ₂ Concentration				
GWB	0.080 ± 0.07	0.186 ± 0.03	0.098 ± 0.01	0.201 ± 0.02
GWB org	0.140 ± 0.09	0.188 ± 0.04	0.112 ± 0.01	0.149 ± 0.03
ERDA-6	0.075 ± 0.04	0.247 ± 0.03	0.189 ± 0.02	0.480 ± 0.04
ERDA-6 org	0.189 ± 0.11	0.126 ± 0.02	0.116 ± 0.02	0.481 ± 0.07
Humid	0.009 ± 0.00	0.021 ± 0.02	0.001 ± 0.00	0.008 ± 0.01
350 ppm CO ₂ Concentration				
GWB	0.189 ± 0.04	0.218 ± 0.02	0.120 ± 0.02	0.231 ± 0.05
GWB org	0.200 ± 0.01	0.232 ± 0.03	0.144 ± 0.03	0.126 ± 0.01
ERDA-6	0.021 ± 0.02	0.176 ± 0.03	0.182 ± 0.05	0.989 ± 0.20
ERDA-6 org	0.022 ± 0.03	0.180 ± 0.05	0.129 ± 0.02	0.444 ± 0.16
Humid	0.005 ± 0.0	0.051 ± 0.03	0.001 ± 0.0	0.000 ± 0.0
1500 ppm CO ₂ Concentration				
GWB	0.239 ± 0.04	0.166 ± 0.05	0.180 ± 0.01	0.289 ± 0.08
GWB org	0.259 ± 0.06	0.221 ± 0.03	0.160 ± 0.01	0.220 ± 0.06
ERDA-6	0.530 ± 0.03	0.577 ± 0.14	0.427 ± 0.09	0.499 ± 0.08
ERDA-6 org	0.258 ± 0.07	0.206 ± 0.04	0.338 ± 0.06	0.427 ± 0.12
Humid	0.000 ± 0.0	0.000 ± 0.0	0.014 ± 0.00	0.009 ± 0.00
3500 ppm CO ₂ Concentration				
GWB	0.397 ± 0.03	0.312 ± 0.01	0.246 ± 0.01	0.316 ± 0.05
GWB org	0.388 ± 0.07	0.264 ± 0.02	0.258 ± 0.04	0.265 ± 0.03
ERDA-6	1.200 ± 0.25	0.924 ± 0.18	0.734 ± 0.08	0.952 ± 0.28
ERDA-6 org	0.650 ± 0.07	0.543 ± 0.09	0.742 ± 0.05	0.788 ± 0.17
Humid	0.008 ± 0.01	0.006 ± 0.01	0.018 ± 0.01	0.004 ± 0.01

Source: Averages calculated from data in Appendix A. Note that negative corrosion rates given in Appendix A are not considered in the calculation of averages.

Table 8 Average Corrosion Rates ($\mu\text{m}/\text{yr}$) for Steel Samples Averaged over all Time Segments

Brine	CO ₂ Concentration (ppm)			
	0	350	1500	3500
GWB	0.141 ± 0.07	0.190 ± 0.05	0.195 ± 0.05	0.318 ± 0.07
GWB org	0.147 ± 0.06	0.175 ± 0.05	0.213 ± 0.06	0.303 ± 0.08
ERDA-6	0.248 ± 0.16	0.342 ± 0.40	0.511 ± 0.11	0.952 ± 0.26
ERDA-6 org	0.228 ± 0.16	0.194 ± 0.18	0.267 ± 0.08	0.645 ± 0.11
Humid	0.010 ± 0.01	0.016 ± 0.03	0.005 ± 0.01	0.010 ± 0.01

Source: Averages calculated from data in Appendix A. Note that negative corrosion rates given in Appendix A are not considered in the calculation of averages.

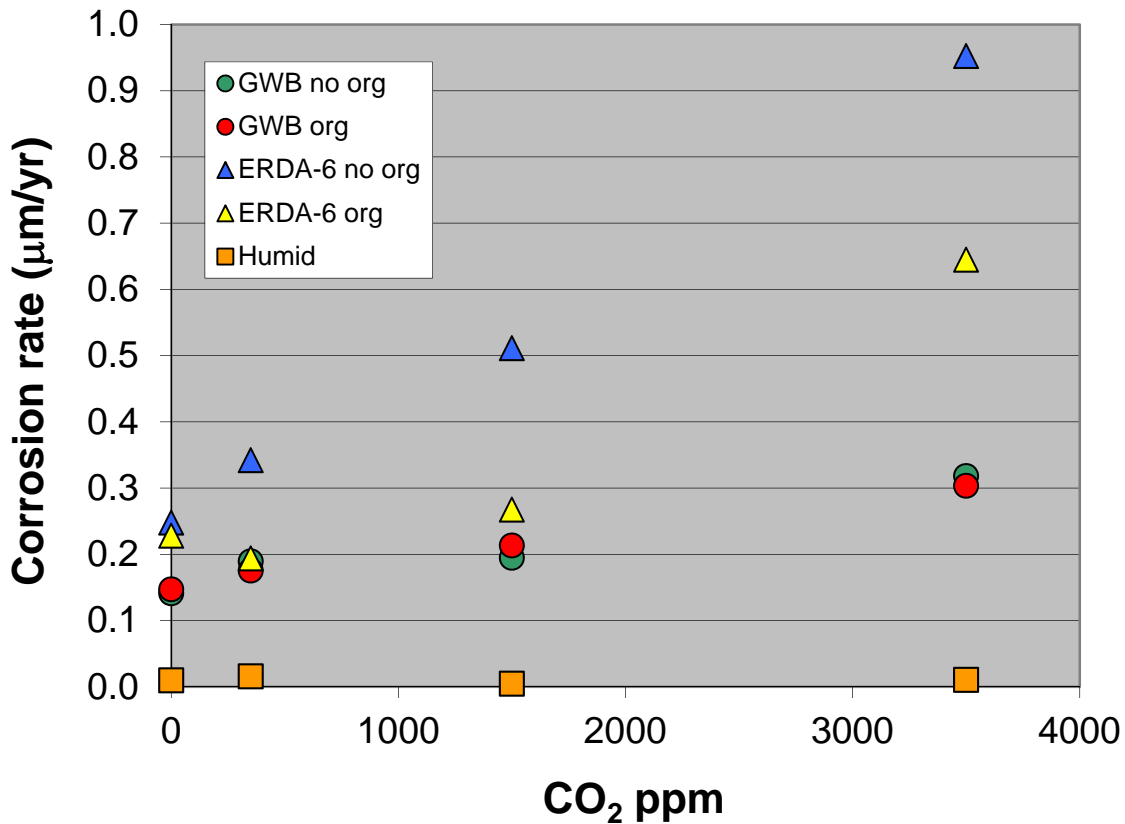


Figure 2 Average corrosion rates for steel coupons in the various brines plotted as a function of the atmospheric CO₂ concentration.

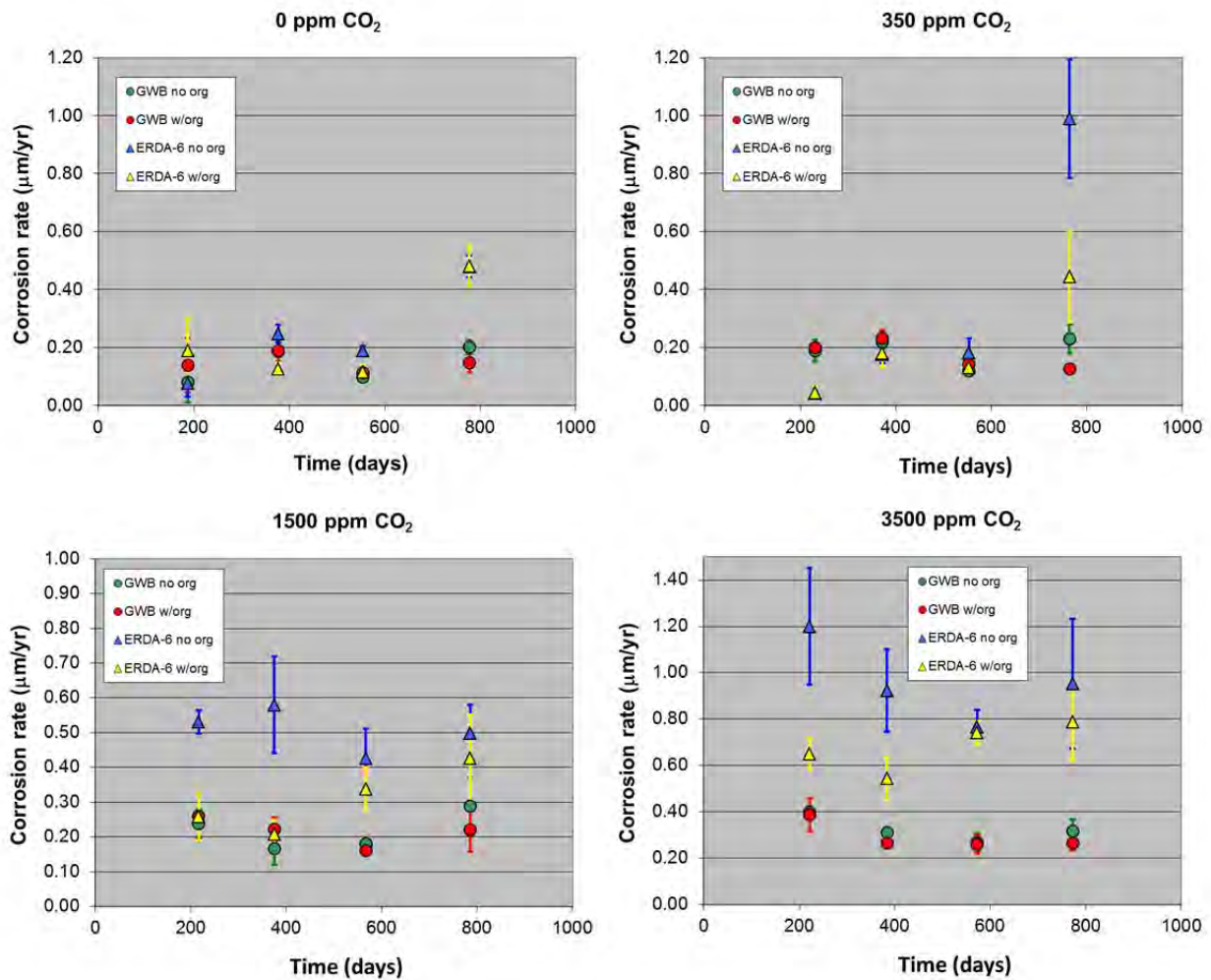


Figure 3 Average corrosion rates for steel coupons in the various brines plotted as a function of time for each of the atmospheric CO₂ concentrations.

4.2 Lead Corrosion Rates

Table 9 gives the lead coupon average corrosion rates calculated from the weight-loss and surface area measurements for each brine type and the humid samples as a function of CO₂ concentration and experimental duration. The average corrosion rates for the different brine types are calculated using the results for both the fully immersed and partially submerged coupons for each brine type. In Table 10 corrosion rates are given that have been averaged over all of the time segments for each brine type and CO₂ concentration.

The average lead corrosion rates presented in Table 10 are plotted as a function of CO₂ concentration in Figure 4. From this plot it can be seen that the data for the lead coupons does not present as clear a picture as for the steel coupons (Figure 2). There may be a dependence on corrosion rates with the CO₂ concentration. Although, given the relatively large standard deviation in the averages (Table 10) it is difficult to determine if there is an actual dependence on CO₂ concentration. Unlike the steel coupons, there does not appear to be significant differences in the corrosion rates between the different brine types. However, there may be some indication that GWB may be more corrosive than the other brines especially at CO₂ concentrations greater than 350 ppm. The humid samples show measureable mass loss regardless of the CO₂ concentration but, it is not certain if the magnitude of the mass loss is within the measurement uncertainty of the graphical analysis method. The porous nature of the lead coupons (see images in Roselle, 2009) is the likely reason for the large variation in the corrosion rate data. The coupon porosity makes it difficult to consistently remove all of the cleaning and rinse solutions used in the weight loss determination. As a result there is more variation in the measured lead weight losses than observed in the steel experiments.

In Figure 5 the corrosion rates presented in Table 9 are plotted as a function of time for each CO₂ concentration and brine type. In these plots it can be seen that the corrosion rates for each CO₂ concentration decline as a function of time. In addition, the corrosion rates for the different brine types appear to reach similar values for all cases except the 3500 ppm CO₂ concentration. The reduction in corrosion rates with time could be an indication that the samples are beginning to show signs of passivation.

Table 9 Average Corrosion Rate ($\mu\text{m}/\text{yr}$) for Lead Samples

Brine	Exposure Duration (months)			
	6	12	18	24
0 ppm CO ₂ Concentration				
GWB	0.541 ± 0.16	0.340 ± 0.16	0.106 ± 0.10	0.152 ± 0.02
GWB org	0.335 ± 0.12	0.411 ± 0.18	0.123 ± 0.08	0.077 ± 0.01
ERDA-6	0.413 ± 0.22	0.300 ± 0.19	0.172 ± 0.14	0.072 ± 0.04
ERDA-6 org	0.319 ± 0.18	0.329 ± 0.21	0.120 ± 0.10	0.068 ± 0.01
Humid	0.061 ± 0.05	0.110 ± 0.02	0.013 ± 0.02	0.006 ± n.d.
350 ppm CO ₂ Concentration				
GWB	0.311 ± 0.33	0.210 ± 0.01	0.142 ± 0.05	0.178 ± 0.03
GWB org	0.363 ± 0.09	0.239 ± 0.08	0.148 ± 0.06	0.102 ± 0.05
ERDA-6	0.194 ± 0.04	0.107 ± 0.14	0.132 ± 0.04	0.110 ± 0.05
ERDA-6 org	0.328 ± 0.06	0.155 ± 0.15	0.131 ± 0.07	0.098 ± 0.06
Humid	n.d.	0.097 ± n.d.	0.046 ± 0.00	0.026 ± n.d.
1500 ppm CO ₂ Concentration				
GWB	0.914 ± 0.82	0.460 ± 0.25	0.193 ± 0.10	0.111 ± 0.03
GWB org	0.950 ± 0.56	0.354 ± 0.21	0.219 ± 0.07	0.123 ± 0.03
ERDA-6	0.469 ± 0.37	0.382 ± 0.30	0.051 ± 0.04	0.123 ± 0.07
ERDA-6 org	0.510 ± 0.31	0.353 ± 0.22	0.124 ± 0.12	0.120 ± 0.05
Humid	0.150 ± 0.05	0.111 ± 0.05	0.048 ± n.d.	0.053 ± 0.01
3500 ppm CO ₂ Concentration				
GWB	0.603 ± 0.28	0.296 ± 0.15	0.213 ± 0.03	0.204 ± 0.10
GWB org	0.625 ± 0.34	0.186 ± 0.05	0.162 ± 0.11	0.256 ± 0.16
ERDA-6	0.729 ± 0.51	0.278 ± 0.23	n.d.	0.062 ± 0.05
ERDA-6 org	0.458 ± 0.17	0.210 ± 0.10	0.039 ± 0.03	0.087 ± 0.06
Humid	0.061 ± 0.02	0.088 ± 0.01	0.069 ± 0.05	0.054 ± 0.03

Source: Averages calculated from data in Appendix A. Note that negative corrosion rates given in Appendix A are not considered in the calculation of averages. Abbreviation n.d. means no data available.

Table 10 Average Corrosion Rates ($\mu\text{m}/\text{yr}$) for Lead Samples Averaged over all Time Segments

Brine	CO ₂ Concentration (ppm)			
	0	350	1500	3500
GWB	0.285 ± 0.21	0.210 ± 0.17	0.522 ± 0.55	0.371 ± 0.24
GWB org	0.247 ± 0.18	0.188 ± 0.11	0.508 ± 0.46	0.324 ± 0.29
ERDA-6	0.239 ± 0.20	0.137 ± 0.07	0.324 ± 0.32	0.536 ± 0.45
ERDA-6 org	0.238 ± 0.18	0.178 ± 0.13	0.329 ± 0.27	0.275 ± 0.21
Humid	0.053 ± 0.05	0.053 ± 0.03	0.114 ± 0.05	0.073 ± 0.03

Source: Averages calculated from data in Appendix A. Note that negative corrosion rates given in Appendix A are not considered in the calculation of averages.

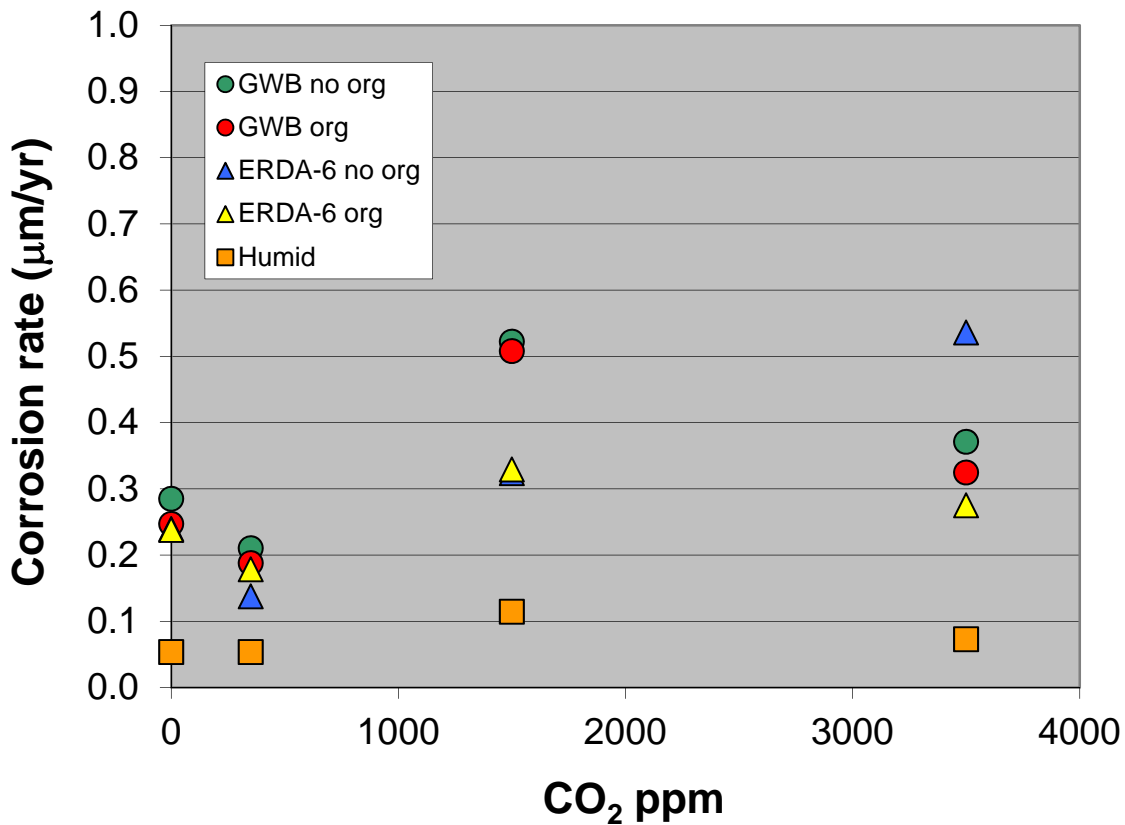


Figure 4 Average corrosion rates for lead coupons in the various brines plotted as a function of the atmospheric CO₂ concentration.

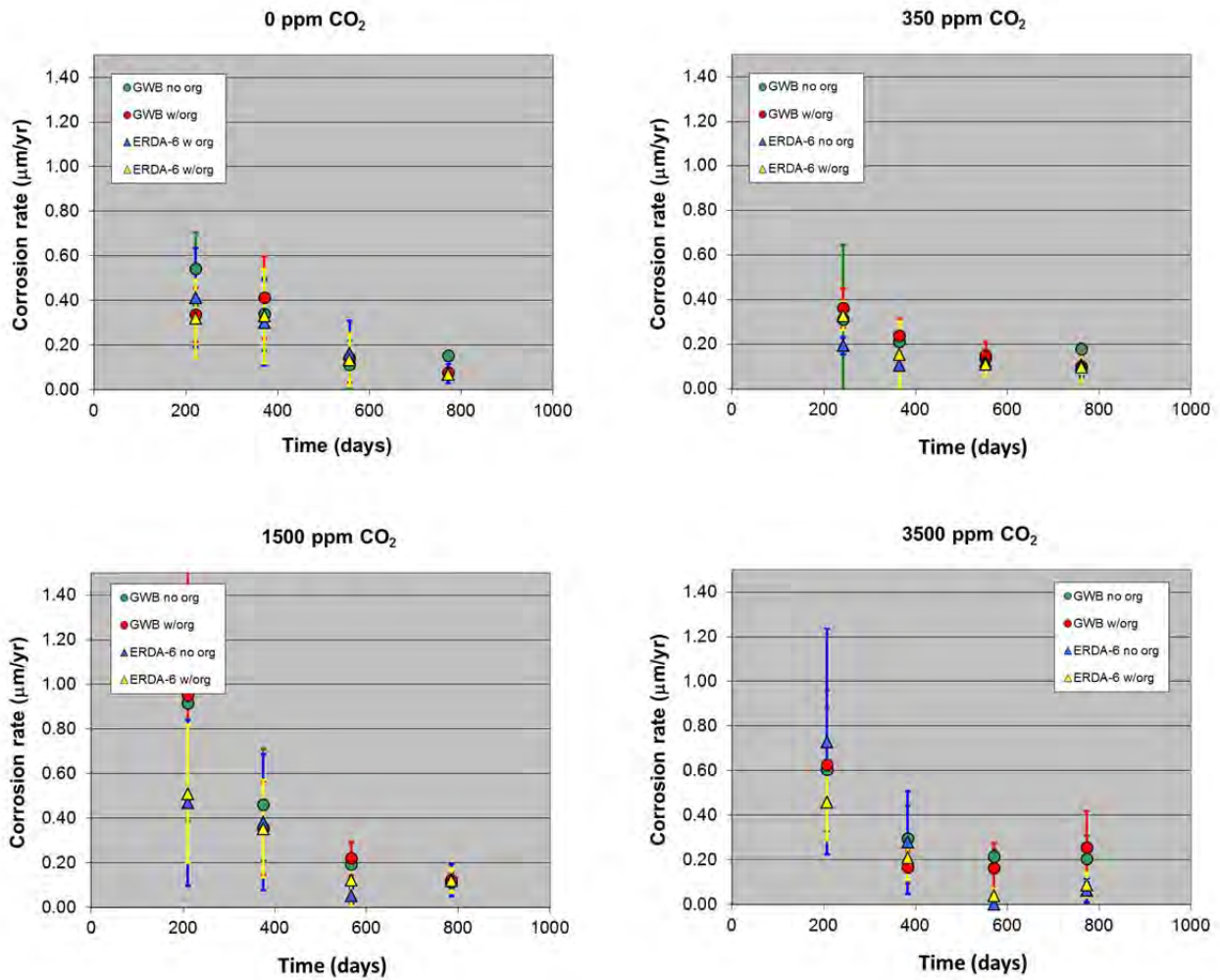


Figure 5 Average corrosion rates for lead coupons in the various brines plotted as a function of time for each of the atmospheric CO₂ concentrations.

4.3 Application of Results to PA Calculations

In the WIPP PA model gas generation is assumed to result from the microbial degradation of CPR materials and the anoxic corrosion steel. The rate of gas generation due to the anoxic corrosion of steel is given by equation PA.68 in Appendix PA of the 2009 CRA (US DOE, 2009):

$$q_{r_{gc}} = (R_{ci} S_{b,eff} + R_{ch} S_g^*) D_s \rho_{Fe} X_c (H_2 | Fe) M_{H_2} \quad (8)$$

where, D_s is the surface area concentration of steel in the repository (m^2 surface area steel/ m^3 disposal volume); M_{H_2} the molecular weight of H_2 ($kg H_2/mol H_2$); R_{ci} the corrosion rate under inundated conditions in the absence of CO_2 (m/s); R_{ch} the corrosion rate under humid conditions (m/s); $S_{b,eff}$ the effective brine saturation due to capillary action in the waste materials; $X_C(H_2|Fe)$ the stoichiometric coefficient for gas generation due to corrosion of steel, i.e., moles of H_2 produced by the corrosion of 1 mole of Fe ($mol H_2/mol Fe$); and ρ_{Fe} is the molar density of steel (mol/m^3).

Three of the variables in Eq. (8) are directly related to the steel corrosion data discussed in this analysis report and can be reevaluated based on the new corrosion experiments. These variables are R_{ci} , the steel corrosion rate under inundated conditions in the absence of CO_2 ; R_{ch} , the corrosion rate under humid conditions and $X_C(H_2|Fe)$, the stoichiometric coefficient for gas generation. These variables correspond to the PA parameters CORRMCO2, HUMCORR, and STOIFX, respectively. The current values used for each of these parameters are given in Table 11.

Table 11 Steel Corrosion PA Parameters from CRA 2009

Parameter	Units	Description	Distribution Type	Distribution Parameters
CORRMCO2	m/s	Rate of anoxic steel corrosion under brine-inundated conditions with no CO_2 present	Uniform	Min = 0 Max = 3.17e-14 Mean = 1.585e-14
HUMCORR	m/s	Rate of anoxic steel corrosion under humid conditions	Constant	0
STOIFX	none	Stoichiometric coefficient for gas generation	Constant	1

Source: WIPP PA Parameter Viewer

The parameter STOIFX represents the stoichiometric coefficient for gas generation. The parameter is currently fixed at a constant value of 1, which implies that one mole of H_2 is produced for each mole of Fe consumed (see Section PA-4.2.5 in Appendix PA, US DOE (2009)). This value is based on observations in the anoxic steel corrosion experiments of Telander and Westermann (1993) that the most likely corrosion product was $Fe(OH)_2$. Although the corrosion products in the current experiments have not been quantitatively identified, there is no indication that they differ significantly from those observed by Telander

and Westermann (1993). Therefore it is recommended that the parameter STOIFX not be changed from its current value.

The anoxic steel corrosion rate under humid conditions is represented by the parameter HUMCORR and is currently set to 0 m/s. The data from the current experiments as shown in Table 7 and Figure 2 support leaving the current value unchanged.

Parameter CORRMCO2 is the most significant corrosion parameter in the gas generation calculations. This parameter represents the anoxic steel corrosion rate for brine-inundated steel in the absence of microbially produced CO₂. There is no consideration for an inundated anoxic steel corrosion rate in the presence of CO₂. Wang and Brush (1996) derived the currently used values for CORRMCO2 (Table 11) based on the experiments of Telander and Westermann (1993). Based on the experimental corrosion data discussed in this report it is recommended that both the distribution type and values for CORRMCO2 be changed. Because the parameter CORRMCO2 represents anoxic corrosion in the absence of CO₂ the experimental data for the 0 ppm conditions are the most appropriate to use for this analysis. As discussed in Section 4.1 the 0 ppm CO₂ corrosion rates remain relatively constant over the entire duration of the experiments and there is little difference between the two brine types. The only anomaly is the ERDA-6 data for the 24 month experiments (see Figure 3). Since these data cannot be definitively excluded from the data set they are also included in the analysis. Based on the form of the data, most samples tightly falling around a mean with one group of outliers, it is suggested that the distribution type be changed from uniform to triangular. The mode of the new distribution is taken as the average of all 0 ppm steel corrosion data except the values for ERDA-6 at 24 months (Table A-1). The maximum value for the new distribution is the average of the 0 ppm CO₂ steel corrosion data for ERDA-6 at 24 months (Table A-1). The minimum of the distribution will remain at 0 m/s. Because the values given in Table A-1 are in units of μm/yr they need to be converted to m/s using the following conversion factor:

$$R_{ci} \text{ (m/s)} = R_{ci} \text{ (}\mu\text{m/yr)} \times (1 \text{ m} / 10^6 \mu\text{m}) \times (1 \text{ yr} / 3.1536 \times 10^7 \text{ s}) \quad (9)$$

The new values for parameter CORRMCO2 given in units of m/s are summarized in Table 12. A plot of the cumulative distribution function (CDF) for the old and new values of parameter CORRMCO2 is given in Figure 6.

Table 12 Revised Steel Corrosion PA Parameter

Parameter	Units	Description	Distribution Type	Distribution Parameters
CORRMCO2	m/s	Rate of anoxic steel corrosion under brine-inundated conditions with no CO ₂ present	Triangular	Min = 0 Max = 1.523e-14 Mode = 4.749e-15 Mean = 6.660e-15 σ = 3.181e-15

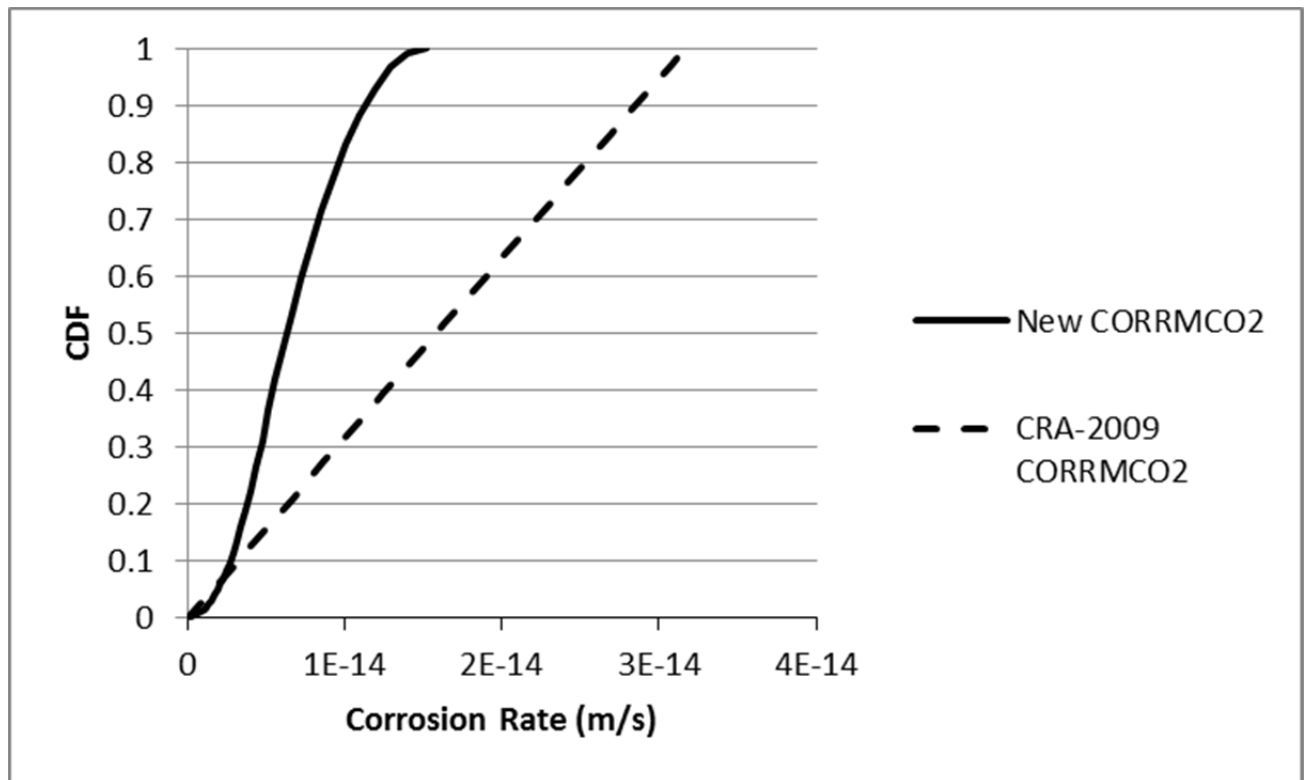


Figure 6 Comparison of the cumulative distribution functions (CDF) for the old and new parameter values for CORRMCO2.

5 *Summary*

This report describes the results of a multi-year study on the corrosion of steel and lead under WIPP-relevant conditions. Analysis of the results from this set of experiments allows the following conclusions to be drawn.

- The corrosion rate of ASTM A1008 low-carbon steel immersed in brine appears to be a function of the CO₂ concentration for all brine types. ERDA-6 brines (with and without organics) appear to be more reactive than the GWB at higher CO₂ concentrations. The addition of organic ligands to the ERDA-6 brine results in significantly less corrosion than the organic free ERDA-6. Corrosion rates for GWB appear to be independent of the presence or absence of organic ligands.
- The corrosion rate of chemical Pb may show a slight dependence of corrosion rates on the CO₂ concentration. However, given the relatively large standard deviation in the averages it is difficult to determine if there is an actual dependence on CO₂ concentration. There does not appear to be any difference in the corrosion rates between the different brine types.
- Steel samples subjected only to humid conditions show no corrosion regardless of the CO₂ concentration. Whereas, humid Pb samples show measureable mass loss regardless of the CO₂ concentration. However, the magnitude of the mass loss may be within the measurement uncertainty of the graphical analysis method.
- Based on the new steel corrosion data it is suggested that the PA parameter CORRMCO2 be changed from a uniform to a triangular distribution. New values for the mode and maximum of the distribution are also given.

6 References

- ASTM (2003) *Standard Practice for Preparing, Cleaning and Evaluation Corrosion Test Specimens*. ASTM G 1 - 03. West Conshohocken, PA: American Society for Testing and Materials (ASTM) International.
- Brush, L.H. (1990) *Test Plan for Laboratory and Modeling Studies of repository and Radionuclide Chemistry for the Waste Isolation Pilot Plant*. SAND90-0266. Albuquerque, NM: Sandia National Laboratories.
- Brush, L.H. (1995) *Systems Priority Method – Iteration 2 Baseline Position Paper: Gas Generation in the Waste Isolation Pilot Plant*. Albuquerque, NM: Sandia National Laboratories.
- Brush, L.H. and Y. Xiong. 2005. *Calculation of Organic-Ligand Concentrations for the WIPP Performance-Assessment Baseline Calculations*. Analysis report, May 4, 2005. Carlsbad, NM: Sandia National Laboratories. ERMS 539635.
- Butcher, B.M. (1990) *Preliminary Evaluation of Potential Engineered Modifications for the Waste Isolation Pilot Plant (WIPP)*. SAND89-3095. Albuquerque, NM: Sandia National Laboratories.
- Brush, L.H. 2005. *Results of Calculations of Actinide Solubilities for the WIPP Performance Assessment Baseline Calculations*. Analysis report, May 18, 2005. Carlsbad, NM: Sandia National Laboratories. ERMS 539800.
- Crawford, B.A. 2005. *Waste Material Densities in TRU Waste Streams from TWBID Revision 2.1 Version 3.13, Data Version D.4.15*. Analysis Report, April 13, 2005. Carlsbad, NM: Los Alamos National Laboratory. ERMS 539323.
- Dunagan, S.C., G.T. Roselle, E.D. Vugrin, and J.L. Long. 2007. *Analysis Report for the Shielded Container Performance Assessment. Revision 1*. Analysis Report, November 7, 2007. Carlsbad, NM: Sandia National Laboratories. ERMS 547358.
- Hertelendy, N.A. 1984. *Rockwell Hanford Operation User's Manual for Remote Handled Transuranic Waste Container*. Rockwell International document no. RHO-RE-MA-7, September, 1984.
- ISO (1991) *Corrosion of Metals and Alloys – Removal of Corrosion Products from Corrosion Test Specimens*. ISO 8407:1991. Geneva, Switzerland: International Organization for Standardization.
- Kubal, M. and F. Panacek. 1995. "Potential-pH Diagram for Fe-H₂O-Citric Acid System", *British Corrosion Journal*, v. 30, no. 4, 309-311.

- MatWeb (2009) *Material Properties for AISI 1008 Steel and Chemical Lead (Pb)*.
<http://www.matweb.com>. ERMS 551896.
- Munson, D.E., R.L. Jones, D.L. Hoag, and J.R. Ball. 1987. *Heated Axisymmetric Pillar Test (Room H): In Situ Data Report (February 1985 – April 1987), Waste Isolation Pilot Plant (WIPP) Thermal/Structural Interactions Program*. SAND87-2488. Albuquerque, NM: Sandia National Laboratories.
- NACE (2000) *Standard Test Method - Laboratory Corrosion Testing of Metals*. TM0169-2000. Houston, TX: National Association of Corrosion Engineers (NACE) International.
- Nemer, M. 2011. “Solubility of $\text{Fe}_2(\text{OH})_3\text{Cl}$ (pure-iron end-member of hibbingite) in NaCl and Na_2SO_4 brines” *Chemical Geology*, v. 280, no. 1-2, 26-32.
- Pletcher, D., D. Sidorin, and B. Hedges. 2005. “A Comparison of the Corrosion of Carbon and 13% Chromium Steels in Oilfield Brines Containing Acetate.” *CO₂ corrosion in Oil and Gas Production Symposium, Proceedings of the NACE Corrosion 2005 Conference held in Houston, TX, April 3-7, 2005*, National Association of Corrosion Engineers (NACE) International, Houston, TX, paper no. 05301.
- Roselle, G.T. (2009) *Iron and Lead Corrosion in WIPP-Relevant Conditions: Six Month Results*. Milestone Report, October 7, 2009. Carlsbad, NM: Sandia National Laboratories. ERMS 546084.
- Roselle, G.T. (2010) *Iron and Lead Corrosion in WIPP-Relevant Conditions: 12 Month Results*. Milestone report, October 14, 2010, Carlsbad, NM: Sandia National Laboratories. ERMS 554383.
- Roselle, G.T. (2011a) *Iron and Lead Corrosion in WIPP-Relevant Conditions: 18 Month Results*. Milestone report, January 5, 2011, Carlsbad, NM: Sandia National Laboratories. ERMS 554715.
- Roselle, G.T. (2011b) *Iron and Lead Corrosion in WIPP-Relevant Conditions: 24 Month Results*. Milestone report, May 3, 2011, Carlsbad, NM: Sandia National Laboratories. ERMS 555246.
- Roselle, G.T. (2012) *Analysis Plan for Determination of Gas Generation Rates from Iron/Lead Corrosion Experiments, AP-159, Rev 0*. ERMS 556297. Carlsbad, NM: Sandia National Laboratories.
- Saltykov, S.N., G.V. Makarov, E.L. Toroptseva, and Y.B. Filatova. 1989. “Anodic Behavior of White Iron Phases in Oxalic Media”. *Protection of Metals*, v. 40, no. 1, 56-61.
- Sankarapavinasam, S., F. Pushpanaden, and M.F. Ahmed. 1989a. “Dicarboxylic Acids as Corrosion Inhibitors for Lead in HClO_4 .” *Bulletin of Electrochemistry*, v. 5, no. 5, 319-323.

- Sankarapavinasam, S., F. Pushpanaden, and M.F. Ahmed. 1989b. "Hydrazine and Substituted Hydrazines as Corrosion Inhibitors for Lead in Acetic Acid." *British Corrosion Journal*, v. 24, no. 1, 39-42.
- Schuhen, M. 2007. Pressure Safety Pressure Package: Mixed Flow Gas Control System for Corrosion Experiments, Rev. 00. Sandia National Laboratories. Carlsbad, NM.
- Sellmer, T. 2007. Final Container Design, Shielded Container. Washington TRU Solutions, Carlsbad, NM. ERMS 547052. Telander, M.R., and R.E. Westerman (1993) *Hydrogen Generation by Metal Corrosion in Simulated Waste Isolation Pilot Plant Environments*. SAND92-7347. Albuquerque, NM: Sandia National Laboratories.
- Telander, M.R., and R.E. Westerman (1997) *Hydrogen Generation by Metal Corrosion in Simulated Waste Isolation Pilot Plant Environments*. SAND96-2538. Albuquerque, NM: Sandia National Laboratories.
- U.S. DOE. 2009. *Title 40 CFR Part 191 Compliance Recertification Application for the Waste Isolation Pilot, Vol. 1-8*. DOE/WIPP 2009-3424. Carlsbad, NM: U.S. Department of Energy Carlsbad Field Office.
- Wall, N.A. and Enos, D. (2006) *Iron and Lead Corrosion in WIPP-Relevant Conditions, TP 06-02, Rev 1*. ERMS 543238. Carlsbad, NM: Sandia National Laboratories.
- Wang, Y. and Brush, L.H. (1996) *Estimates of Gas-Generation Parameters for the Long-Term WIPP Performance Assessment*. Memo to Martin S. Tierney, January 26, 1996. ERMS 231943. Carlsbad, NM: Sandia National Laboratories.

7 *Appendix A*

Table A-1 lists the exposure duration, initial weight, final weight, weight loss, surface area and calculated corrosion rate for each steel coupon. The equivalent data for the lead coupons is given in Table A-2. The reported surface data are taken from Roselle (2009, 2010, 2011a, 2011b) for the 6, 12, 18 and 24 month experiments, respectively. Corrosion rates are calculated according to Equation (7) given in Section 3.5.

Table A- 1 Summary of Steel Coupon Corrosion Rate Data

Test ID	Coupon	Duration (hours)	Initial Wt (g)	Final Wt (g) (Calculated)	Weight Loss (mg)	Surface Area (cm ²)	Corrosion Rate (µm/yr)
Fe-G-0000-6-1f	87	4488	20.2056	20.2046	1.0	41.629	0.060
Fe-G-0000-6-3f	89	4488	20.0899	20.0887	1.2	41.663	0.071
Fe-G-0000-6-1p	90	4488	20.3926	20.3909	1.7	23.751	0.177
Fe-G-0000-6-2p	91	4488	19.3842	19.3841	0.1	23.918	0.010
Fe-Go-0000-6-2f	94	4488	19.7502	19.7471	3.1	41.625	0.185
Fe-Go-0000-6-3f	95	4488	19.8811	19.8769	4.2	41.505	0.251
Fe-Go-0000-6-2p	97	4488	18.4242	18.4235	0.7	24.389	0.071
Fe-Go-0000-6-3p	98	4488	18.5963	18.5958	0.5	24.033	0.052
Fe-E-0000-6-1f	99	4488	18.8115	18.8113	0.2	41.709	0.012
Fe-E-0000-6-2f	100	4488	19.2114	19.2097	1.7	41.641	0.101
Fe-E-0000-6-1p	102	4488	20.2687	20.2679	0.8	25.583	0.078
Fe-E-0000-6-2p	103	4488	20.0235	20.0224	1.1	24.773	0.110
Fe-Eo-0000-6-2f	106	4488	20.1808	20.1791	1.7	41.446	0.102
Fe-Eo-0000-6-3f	107	4488	20.2049	20.2034	1.5	41.464	0.090
Fe-Eo-0000-6-1p	108	4488	20.2672	20.2645	2.7	24.634	0.272
Fe-Eo-0000-6-2p	109	4488	20.1048	20.1019	2.9	24.473	0.294
Fe-Atm-0000-6-1	111	4488	19.4744	19.4742	0.2	41.457	0.012
Fe-Atm-0000-6-2	112	4488	19.6178	19.6177	0.1	41.534	0.006
Fe-G-0350-6-1f	114	5544	19.8297	19.8248	4.9	41.594	0.236
Fe-G-0350-6-2f	115	5544	20.0005	19.9970	3.5	41.617	0.169
Fe-G-0350-6-1p	117	5544	18.5283	18.5259	2.4	23.976	0.201
Fe-G-0350-6-2p	118	5544	18.7634	18.7616	1.8	24.272	0.149
Fe-Go-0350-6-1f	120	5544	19.3063	19.3021	4.2	41.405	0.204
Fe-Go-0350-6-2f	121	5544	20.4382	20.4339	4.3	41.634	0.207
Fe-Go-0350-6-1p	123	5544	20.1489	20.1465	2.4	24.181	0.199
Fe-Go-0350-6-2p	124	5544	20.2366	20.2343	2.3	24.496	0.188
Fe-E-0350-6-1f	126	5544	20.1509	20.1499	1.0	41.561	0.048
Fe-E-0350-6-2f	127	5544	20.2231	20.2224	0.7	41.526	0.034
Fe-E-0350-6-1p	129	5544	20.0739	20.0758	-1.9	23.843	-0.160
Fe-E-0350-6-2p	130	5544	20.3403	20.3406	-0.3	24.270	-0.025
Fe-Eo-0350-6-1f	132	5544	19.6018	19.6012	0.6	41.502	0.029
Fe-Eo-0350-6-2f	133	5544	19.7301	19.7289	1.2	41.613	0.058
Fe-Eo-0350-6-1p	135	5544	19.9139	19.9141	-0.2	23.204	-0.017
Fe-Eo-0350-6-2p	136	5544	18.3987	18.3992	-0.5	23.356	-0.043
Fe-Atm-0350-6-1	138	5544	18.7107	18.7113	-0.6	41.535	-0.029
Fe-Atm-0350-6-2	139	5544	18.8829	18.8828	0.1	41.375	0.005
Fe-G-1500-6-2f	307	5208	20.4468	20.4433	3.5	41.756	0.179
Fe-G-1500-6-3f	308	5208	20.4428	20.4378	5.0	41.781	0.256
Fe-G-1500-6-2p	310	5208	20.6744	20.6714	3.0	24.858	0.258
Fe-G-1500-6-3p	311	5208	20.0198	20.0168	3.0	24.512	0.262
Fe-Go-1500-6-2f	313	5208	20.2360	20.2303	5.7	41.770	0.292

Test ID	Coupon	Duration (hours)	Initial Wt (g)	Final Wt (g) (Calculated)	Weight Loss (mg)	Surface Area (cm ²)	Corrosion Rate (µm/yr)
Fe-Go-1500-6-3f	314	5208	20.4547	20.4492	5.5	41.711	0.282
Fe-Go-1500-6-2p	316	5208	19.3890	19.3872	1.8	23.589	0.163
Fe-Go-1500-6-3p	317	5208	19.6472	19.6440	3.2	22.720	0.301
Fe-E-1500-6-2f	319	5208	20.1540	20.1434	10.6	41.838	0.541
Fe-E-1500-6-3f	320	5208	20.3862	20.3752	11.0	41.611	0.565
Fe-E-1500-6-2p	322	5208	18.8133	18.8081	5.2	22.927	0.485
Fe-E-1500-6-3p	323	5208	19.0999	19.0942	5.7	23.024	0.529
Fe-Eo-1500-6-2f	325	5208	19.9421	19.9369	5.2	41.723	0.266
Fe-Eo-1500-6-3f	326	5208	20.2902	20.2845	5.7	41.636	0.293
Fe-Eo-1500-6-2p	328	5208	19.8855	19.8838	1.7	22.565	0.161
Fe-Eo-1500-6-3p	329	5208	19.8942	19.8909	3.3	22.588	0.312
Fe-Atm-1500-6-2	331	5208	20.4723	20.4723	0.0	41.612	0.000
Fe-Atm-1500-6-3	332	5208	20.4969	20.4971	-0.2	41.606	-0.010
Fe-G-3500-6-2f	416	5328	19.9560	19.9487	7.3	41.449	0.368
Fe-G-3500-6-3f	417	5328	19.9064	19.8989	7.5	41.443	0.378
Fe-G-3500-6-1p	418	5328	19.6738	19.6694	4.4	21.659	0.424
Fe-G-3500-6-2p	419	5328	19.5823	19.5780	4.3	21.521	0.417
Fe-Go-3500-6-2f	423	5328	19.1900	19.1833	6.7	41.317	0.339
Fe-Go-3500-6-3f	424	5328	19.1962	19.1893	6.9	41.316	0.349
Fe-Go-3500-6-1p	425	5328	19.2495	19.2444	5.1	21.545	0.494
Fe-Go-3500-6-2p	426	5328	20.7596	20.7557	3.9	22.001	0.370
Fe-E-3500-6-2f	430	5328	19.5257	19.5020	23.7	41.442	1.194
Fe-E-3500-6-3f	431	5328	21.0621	21.0447	17.4	41.617	0.873
Fe-E-3500-6-2p	433	5328	20.5718	20.5580	13.8	23.045	1.251
Fe-E-3500-6-3p	434	5328	20.3482	20.3325	15.7	22.135	1.481
Fe-Eo-3500-6-1f	435	5328	20.2338	20.2212	12.6	41.597	0.633
Fe-Eo-3500-6-2f	436	5328	20.5356	20.5236	12.0	41.420	0.605
Fe-Eo-3500-6-1p	438	5328	20.2190	20.2122	6.8	23.304	0.609
Fe-Eo-3500-6-2p	439	5328	20.1788	20.1707	8.1	22.475	0.753
Fe-Atm-3500-6-1	441	5328	20.0863	20.0860	0.3	41.368	0.015
Fe-Atm-3500-6-2	442	5328	20.0771	20.0776	-0.5	41.502	-0.025
Fe-G-0000-12-1f	60	9048	19.3011	19.2959	5.2	41.666	0.153
Fe-G-0000-12-2f	61	9048	20.5591	20.5512	7.9	41.763	0.233
Fe-G-0000-12-1p	63	9048	20.3449	20.3417	3.2	23.495	0.168
Fe-G-0000-12-2p	64	9048	20.3755	20.3719	3.6	23.320	0.190
Fe-Go-0000-12-1f	66	9048	20.1063	20.0992	7.1	41.589	0.210
Fe-Go-0000-12-2f	67	9048	20.1960	20.1917	4.3	41.678	0.127
Fe-Go-0000-12-1p	69	9048	20.0246	20.0198	4.8	27.610	0.214
Fe-Go-0000-12-2p	70	9048	20.2859	20.2817	4.2	25.698	0.201
Fe-E-0000-12-1f	72	9048	19.5601	19.5513	8.8	41.656	0.260
Fe-E-0000-12-2f	73	9048	19.5790	19.5695	9.5	41.516	0.281
Fe-E-0000-12-1p	75	9048	19.8687	19.8646	4.1	24.408	0.207
Fe-E-0000-12-2p	76	9048	18.4585	18.4537	4.8	24.385	0.242
Fe-Eo-0000-12-1f	78	9048	18.6946	18.6899	4.7	41.580	0.139
Fe-Eo-0000-12-2f	79	9048	18.8659	18.8609	5.0	41.453	0.148

Test ID	Coupon	Duration (hours)	Initial Wt (g)	Final Wt (g) (Calculated)	Weight Loss (mg)	Surface Area (cm ²)	Corrosion Rate (µm/yr)
Fe-Eo-0000-12-1p	81	9048	20.5837	20.5817	2.0	24.021	0.102
Fe-Eo-0000-12-2p	82	9048	20.4241	20.4218	2.3	24.833	0.114
Fe-Atm-0000-12-1	84	9048	20.2808	20.2805	0.3	41.748	0.009
Fe-Atm-0000-12-2	85	9048	20.2084	20.2073	1.1	41.827	0.032
Fe-G-0350-12-2f	190	8928	20.1010	20.0934	7.6	41.452	0.229
Fe-G-0350-12-3f	191	8928	19.6566	19.6502	6.4	41.453	0.192
Fe-G-0350-12-1p	192	8928	19.6893	19.6850	4.3	22.433	0.239
Fe-G-0350-12-2p	202	8928	20.1691	20.1651	4.0	23.307	0.214
Fe-Go-0350-12-2f	205	8928	19.9700	19.9625	7.5	41.706	0.224
Fe-Go-0350-12-3f	206	8928	20.4860	20.4784	7.6	41.568	0.228
Fe-Go-0350-12-1p	207	8928	20.5629	20.5574	5.5	25.466	0.269
Fe-Go-0350-12-2p	208	8928	20.5510	20.5469	4.1	24.809	0.206
Fe-E-0350-12-1f	210	8928	20.7959	20.7910	4.9	41.537	0.147
Fe-E-0350-12-3f	212	8928	20.4249	20.4192	5.7	41.561	0.171
Fe-E-0350-12-1p	213	8928	20.4342	20.4307	3.5	25.757	0.169
Fe-E-0350-12-2p	214	8928	20.5784	20.5740	4.4	25.133	0.218
Fe-Eo-0350-12-2f	217	8928	19.8691	19.8647	4.4	41.595	0.132
Fe-Eo-0350-12-3f	218	8928	19.9675	19.9621	5.4	41.579	0.162
Fe-Eo-0350-12-2p	220	8928	20.5543	20.5494	4.9	24.663	0.248
Fe-Eo-0350-12-3p	221	8928	18.5283	18.5247	3.6	25.007	0.179
Fe-Atm-0350-12-1	222	8928	18.8982	18.8972	1.0	41.291	0.030
Fe-Atm-0350-12-2	223	8928	19.0679	19.0655	2.4	41.427	0.072
Fe-G-1500-12-2f	280	9048	20.0104	20.0037	6.7	41.592	0.198
Fe-G-1500-12-3f	281	9048	20.5189	20.5123	6.6	41.534	0.195
Fe-G-1500-12-2p	283	9048	20.5013	20.4980	3.3	23.525	0.173
Fe-G-1500-12-3p	284	9048	20.5887	20.5868	1.9	23.885	0.098
Fe-Go-1500-12-2f	286	9048	20.0247	20.0169	7.8	41.620	0.230
Fe-Go-1500-12-3f	287	9048	20.1628	20.1548	8.0	41.505	0.237
Fe-Go-1500-12-2p	289	9048	20.4700	20.4669	3.1	22.377	0.170
Fe-Go-1500-12-3p	290	9048	20.6715	20.6671	4.4	22.094	0.245
Fe-E-1500-12-2f	292	9048	19.6078	19.5819	25.9	41.565	0.766
Fe-E-1500-12-3f	293	9048	19.8102	19.7953	14.9	42.073	0.436
Fe-E-1500-12-2p	295	9048	20.3754	20.3639	11.5	24.876	0.569
Fe-E-1500-12-3p	296	9048	18.6232	18.6121	11.1	25.442	0.537
Fe-Eo-1500-12-2f	298	9048	19.1280	19.1211	6.9	41.791	0.203
Fe-Eo-1500-12-3f	299	9048	19.5338	19.5266	7.2	41.571	0.213
Fe-Eo-1500-12-2p	301	9048	20.2896	20.2865	3.1	24.901	0.153
Fe-Eo-1500-12-3p	302	9048	20.1619	20.1568	5.1	24.639	0.255
Fe-Atm-1500-12-2	304	9048	20.0619	20.0639	-2.0	41.650	-0.059
Fe-Atm-1500-12-3	305	9048	19.9653	19.9669	-1.6	41.694	-0.047
Fe-G-3500-12-1f	388	9216	20.2823	20.2717	10.6	41.679	0.307
Fe-G-3500-12-2f	389	9216	20.4266	20.4162	10.4	41.613	0.302
Fe-G-3500-12-1p	391	9216	19.5371	19.5317	5.4	20.603	0.316
Fe-G-3500-12-2p	392	9216	19.7584	19.7525	5.9	22.200	0.321
Fe-Go-3500-12-1f	394	9216	20.1677	20.1592	8.5	41.626	0.247

Test ID	Coupon	Duration (hours)	Initial Wt (g)	Final Wt (g) (Calculated)	Weight Loss (mg)	Surface Area (cm ²)	Corrosion Rate (µm/yr)
Fe-Go-3500-12-2f	395	9216	20.3568	20.3479	8.9	41.664	0.258
Fe-Go-3500-12-1p	397	9216	19.0914	19.0857	5.7	24.076	0.286
Fe-Go-3500-12-2p	398	9216	19.2442	19.2390	5.2	23.481	0.267
Fe-E-3500-12-1f	400	9216	19.9873	19.9496	37.7	41.510	1.097
Fe-E-3500-12-2f	401	9216	20.5452	20.5217	23.5	41.475	0.684
Fe-E-3500-12-1p	403	9216	19.7813	19.7641	17.2	22.850	0.909
Fe-E-3500-12-2p	404	9216	19.4440	19.4252	18.8	22.597	1.005
Fe-Eo-3500-12-1f	406	9216	20.9043	20.8890	15.3	41.639	0.444
Fe-Eo-3500-12-2f	407	9216	20.6746	20.6577	16.9	41.466	0.492
Fe-Eo-3500-12-1p	409	9216	20.2286	20.2170	11.6	23.658	0.592
Fe-Eo-3500-12-2p	410	9216	20.0146	20.0024	12.2	22.850	0.645
Fe-Atm-3500-12-1	412	9192	20.4797	20.4793	0.4	41.505	0.012
Fe-Atm-3500-12-2	413	9192	20.1305	20.1305	0.0	41.386	0.000
Fe-G-0000-18-2f	34	13296	19.5493	19.5440	5.3	41.520	0.107
Fe-G-0000-18-3f	35	13296	19.6833	19.6788	4.5	41.645	0.090
Fe-G-0000-18-2p	37	13296	18.3932	18.3903	2.9	23.433	0.104
Fe-G-0000-18-3p	38	13296	18.4550	18.4525	2.5	22.555	0.093
Fe-Go-0000-18-2f	40	13296	18.9886	18.9827	5.9	41.499	0.119
Fe-Go-0000-18-3f	41	13296	20.4180	20.4122	5.8	41.621	0.117
Fe-Go-0000-18-2p	43	13296	20.3030	20.3003	2.7	24.835	0.091
Fe-Go-0000-18-3p	44	13296	20.4383	20.4347	3.6	24.445	0.123
Fe-E-0000-18-2f	46	13296	20.1818	20.1725	9.3	41.723	0.187
Fe-E-0000-18-3f	47	13296	20.2995	20.2895	10.0	41.588	0.201
Fe-E-0000-18-2p	49	13296	20.2017	20.1968	4.9	24.484	0.167
Fe-E-0000-18-3p	50	13296	20.0687	20.0630	5.7	23.666	0.202
Fe-Eo-0000-18-2f	52	13296	19.6660	19.6597	6.3	41.565	0.127
Fe-Eo-0000-18-3f	53	13296	19.7653	19.7600	5.3	41.755	0.106
Fe-Eo-0000-18-2p	55	13296	20.0585	20.0557	2.8	26.349	0.089
Fe-Eo-0000-18-3p	56	13296	18.4668	18.4624	4.4	25.838	0.143
Fe-Atm-0000-18-2	58	13296	18.7299	18.7298	0.1	41.542	0.002
Fe-Atm-0000-18-3	59	13296	18.8844	18.8844	0.0	41.520	0.000
Fe-G-0350-18-2f	169	13272	20.0624	20.0559	6.5	41.643	0.131
Fe-G-0350-18-3f	170	13272	20.1873	20.1811	6.2	41.722	0.125
Fe-G-0350-18-2p	172	13272	19.6613	19.6586	2.7	23.280	0.097
Fe-G-0350-18-3p	173	13272	19.7186	19.7151	3.5	22.784	0.129
Fe-Go-0350-18-2f	175	13272	19.7910	19.7857	5.3	41.595	0.107
Fe-Go-0350-18-3f	176	13272	18.6358	18.6286	7.2	41.138	0.147
Fe-Go-0350-18-2p	178	13272	18.7196	18.7155	4.1	24.054	0.143
Fe-Go-0350-18-3p	179	13272	18.8799	18.8753	4.6	21.637	0.178
Fe-E-0350-18-2f	181	13272	20.5586	20.5469	11.7	41.665	0.235
Fe-E-0350-18-3f	182	13272	20.3932	20.3826	10.6	41.606	0.214
Fe-E-0350-18-2p	184	13272	20.0962	20.0920	4.2	24.550	0.143
Fe-E-0350-18-3p	185	13272	19.9873	19.9836	3.7	22.896	0.135
Fe-Eo-0350-18-2f	187	13272	20.1792	20.1718	7.4	41.548	0.149
Fe-Eo-0350-18-3f	188	13272	20.2219	20.2150	6.9	41.554	0.139

Test ID	Coupon	Duration (hours)	Initial Wt (g)	Final Wt (g) (Calculated)	Weight Loss (mg)	Surface Area (cm ²)	Corrosion Rate (µm/yr)
Fe-Eo-0350-18-2p	195	13272	19.6885	19.6853	3.2	21.356	0.126
Fe-Eo-0350-18-3p	196	13272	18.7094	18.7066	2.8	22.799	0.103
Fe-Atm-0350-18-2	198	13272	18.7610	18.7611	-0.1	41.231	-0.002
Fe-Atm-0350-18-3	201	13272	20.1683	20.1682	0.1	41.496	0.002
Fe-G-1500-18-2f	253	13608	18.8198	18.8100	9.8	41.343	0.194
Fe-G-1500-18-3f	254	13608	19.0262	19.0176	8.6	41.438	0.170
Fe-G-1500-18-2p	256	13608	19.3590	19.3532	5.8	25.973	0.183
Fe-G-1500-18-3p	257	13608	19.5622	19.5568	5.4	25.480	0.173
Fe-Go-1500-18-2f	259	13608	19.6236	19.6152	8.4	41.581	0.165
Fe-Go-1500-18-3f	260	13608	19.8384	19.8305	7.9	41.454	0.156
Fe-Go-1500-18-2p	262	13608	19.7987	19.7936	5.1	24.180	0.172
Fe-Go-1500-18-3p	263	13608	19.6969	19.6924	4.5	24.944	0.148
Fe-E-1500-18-2f	265	13608	19.9768	19.9574	19.4	41.614	0.381
Fe-E-1500-18-3f	266	13608	19.4376	19.4200	17.6	41.380	0.348
Fe-E-1500-18-2p	268	13608	19.5566	19.5406	16.0	24.120	0.542
Fe-E-1500-18-3p	269	13608	19.6998	19.6863	13.5	25.337	0.436
Fe-Eo-1500-18-2f	271	13608	19.0806	19.0613	19.3	41.474	0.381
Fe-Eo-1500-18-3f	272	13608	19.1743	19.1541	20.2	41.347	0.400
Fe-Eo-1500-18-2p	274	13608	19.2944	19.2858	8.6	23.462	0.300
Fe-Eo-1500-18-3p	275	13608	19.5771	19.5693	7.8	23.344	0.273
Fe-Atm-1500-18-2	277	13608	20.2048	20.2038	1.0	41.525	0.020
Fe-Atm-1500-18-3	278	13608	20.0311	20.0307	0.4	41.508	0.008
Fe-G-3500-18-2f	362	13752	20.3139	20.3016	12.3	41.589	0.239
Fe-G-3500-18-3f	363	13752	20.3431	20.3308	12.3	41.571	0.239
Fe-G-3500-18-2p	365	13752	20.6158	20.6076	8.2	25.146	0.264
Fe-G-3500-18-3p	366	13752	19.5118	19.5043	7.5	25.049	0.242
Fe-Go-3500-18-2f	368	13752	19.9349	19.9233	11.6	41.451	0.226
Fe-Go-3500-18-3f	369	13752	20.1843	20.1725	11.8	41.459	0.230
Fe-Go-3500-18-2p	371	13752	18.7512	18.7430	8.2	24.035	0.276
Fe-Go-3500-18-3p	372	13752	19.0172	19.0083	8.9	24.077	0.299
Fe-E-3500-18-2f	374	13752	19.6811	19.6434	37.7	41.404	0.737
Fe-E-3500-18-3f	375	13752	19.9213	19.8820	39.3	41.510	0.766
Fe-E-3500-18-2p	377	13752	20.1881	20.1636	24.5	24.676	0.803
Fe-E-3500-18-3p	378	13752	20.0073	19.9879	19.4	24.994	0.628
Fe-Eo-3500-18-2f	380	13752	19.8498	19.8118	38.0	41.637	0.739
Fe-Eo-3500-18-3f	381	13752	20.5335	20.4978	35.7	41.674	0.693
Fe-Eo-3500-18-2p	383	13752	20.4598	20.4359	23.9	23.813	0.812
Fe-Eo-3500-18-3p	384	13752	20.5520	20.5301	21.9	24.503	0.723
Fe-Atm-3500-18-2	386	13752	20.0792	20.0788	0.4	41.475	0.008
Fe-Atm-3500-18-3	387	13752	20.2290	20.2276	1.4	41.596	0.027
Fe-G-0000-24-1f	1	18648	20.6240	20.6087	15.3	41.776	0.219
Fe-G-0000-24-2f	2	18648	20.5841	20.5714	12.7	41.703	0.182
Fe-G-0000-24-1p	9	18648	20.4679	20.4582	9.7	25.782	0.225
Fe-G-0000-24-2p	10	18648	20.5272	20.5195	7.7	25.798	0.178
Fe-Go-0000-24-1f	12	18648	20.2285	20.2192	9.3	41.804	0.133

Test ID	Coupon	Duration (hours)	Initial Wt (g)	Final Wt (g) (Calculated)	Weight Loss (mg)	Surface Area (cm ²)	Corrosion Rate (µm/yr)
Fe-Go-0000-24-2f	13	18648	20.2769	20.2694	7.5	41.830	0.107
Fe-Go-0000-24-1p	15	18648	20.3798	20.3729	6.9	23.093	0.178
Fe-Go-0000-24-2p	16	18648	19.5429	19.5365	6.4	21.650	0.176
Fe-E-0000-24-1f	18	18648	19.6337	19.6031	30.6	41.593	0.439
Fe-E-0000-24-2f	19	18648	19.7774	19.7450	32.4	41.553	0.465
Fe-E-0000-24-1p	21	18648	20.2797	20.2568	22.9	27.898	0.490
Fe-E-0000-24-2p	22	18648	20.1809	20.1559	25.0	28.443	0.525
Fe-Eo-0000-24-1f	24	18648	19.8657	19.8324	33.3	41.775	0.476
Fe-Eo-0000-24-2f	25	18648	19.8175	19.7891	28.4	41.598	0.407
Fe-Eo-0000-24-1p	27	18648	20.1286	20.1052	23.4	30.197	0.462
Fe-Eo-0000-24-2p	28	18648	20.0979	20.0719	26.0	26.818	0.579
Fe-Atm-0000-24-1	30	18648	20.0973	20.0963	1.0	41.512	0.014
Fe-Atm-0000-24-2	31	18648	19.3834	19.3833	0.1	41.450	0.001
Fe-G-0350-24-2f	142	18336	20.3932	20.3805	12.7	41.538	0.186
Fe-G-0350-24-3f	143	18336	20.1383	20.1251	13.2	41.514	0.193
Fe-G-0350-24-2p	145	18336	20.2947	20.2843	10.4	24.981	0.253
Fe-G-0350-24-3p	146	18336	20.1988	20.1865	12.3	25.644	0.291
Fe-Go-0350-24-2f	148	18336	20.1712	20.1632	8.0	41.674	0.117
Fe-Go-0350-24-3f	149	18336	20.0060	19.9978	8.2	41.561	0.120
Fe-Go-0350-24-2p	151	18336	19.4084	19.4029	5.5	24.496	0.136
Fe-Go-0350-24-3p	152	18336	19.5225	19.5172	5.3	24.325	0.132
Fe-E-0350-24-2f	154	18336	19.5756	19.5226	53.0	41.430	0.776
Fe-E-0350-24-3f	155	18336	19.8205	19.7595	61.0	41.513	0.892
Fe-E-0350-24-2p	157	18336	18.3299	18.2938	36.1	21.084	1.039
Fe-E-0350-24-3p	158	18336	18.5795	18.5345	45.0	21.861	1.249
Fe-Eo-0350-24-2f	160	18336	19.1297	19.0906	39.1	41.698	0.569
Fe-Eo-0350-24-3f	161	18336	20.4086	20.3683	40.3	41.597	0.588
Fe-Eo-0350-24-2p	163	18336	20.2446	20.2320	12.6	24.924	0.307
Fe-Eo-0350-24-3p	164	18336	20.2056	20.1929	12.7	24.842	0.310
Fe-Atm-0350-24-2	166	18336	20.2371	20.2373	-0.2	41.629	-0.003
Fe-Atm-0350-24-3	167	18336	20.2530	20.2531	-0.1	41.557	-0.001
Fe-G-1500-24-2f	226	18864	18.6941	18.6785	15.6	41.205	0.223
Fe-G-1500-24-3f	227	18864	19.2821	19.2658	16.3	41.414	0.232
Fe-G-1500-24-2p	229	18864	19.0517	19.0343	17.4	25.421	0.404
Fe-G-1500-24-3p	230	18864	19.0467	19.0337	13.0	25.965	0.295
Fe-Go-1500-24-2f	232	18864	19.9854	19.9734	12.0	41.579	0.170
Fe-Go-1500-24-3f	233	18864	19.8149	19.8035	11.4	41.523	0.162
Fe-Go-1500-24-2p	235	18864	20.0636	20.0516	12.0	25.633	0.276
Fe-Go-1500-24-3p	236	18864	19.8832	19.8712	12.0	25.944	0.273
Fe-E-1500-24-2f	238	18864	19.9648	19.9353	29.5	41.521	0.419
Fe-E-1500-24-3f	239	18864	20.0428	20.0118	31.0	41.612	0.439
Fe-E-1500-24-2p	241	18864	19.3937	19.3707	23.0	24.266	0.559
Fe-E-1500-24-3p	242	18864	19.6989	19.6750	23.9	24.399	0.578
Fe-Eo-1500-24-2f	244	18864	19.7472	19.7086	38.6	41.567	0.548
Fe-Eo-1500-24-3f	245	18864	19.9761	19.9400	36.1	41.664	0.511

Test ID	Coupon	Duration (hours)	Initial Wt (g)	Final Wt (g) (Calculated)	Weight Loss (mg)	Surface Area (cm ²)	Corrosion Rate (µm/yr)
Fe-Eo-1500-24-2p	247	18864	19.0860	19.0706	15.4	24.766	0.367
Fe-Eo-1500-24-3p	248	18864	18.9766	18.9647	11.9	25.026	0.281
Fe-Atm-1500-24-2	250	18864	19.5200	19.5192	0.8	41.518	0.011
Fe-Atm-1500-24-3	251	18864	18.5320	18.5315	0.5	41.308	0.007
Fe-G-3500-24-2f	334	18552	20.5720	20.5448	27.2	41.591	0.392
Fe-G-3500-24-3f	335	18552	20.6391	20.6188	20.3	41.619	0.293
Fe-G-3500-24-2p	337	18552	20.2438	20.2309	12.9	25.609	0.302
Fe-G-3500-24-3p	338	18552	20.2790	20.2665	12.5	27.120	0.276
Fe-Go-3500-24-2f	340	18552	20.6052	20.5893	15.9	41.764	0.228
Fe-Go-3500-24-3f	341	18552	19.5010	19.4832	17.8	41.423	0.258
Fe-Go-3500-24-2p	343	18552	19.8981	19.8869	11.2	24.688	0.272
Fe-Go-3500-24-3p	345	18552	20.4076	20.3950	12.6	24.956	0.303
Fe-E-3500-24-2f	347	18552	18.9234	18.8484	75.0	41.348	1.088
Fe-E-3500-24-3f	348	18552	19.1652	19.1028	62.4	41.548	0.901
Fe-E-3500-24-2p	350	18552	19.9314	19.8818	49.6	24.136	1.233
Fe-E-3500-24-3p	351	18552	20.2387	20.2152	23.5	24.066	0.586
Fe-Eo-3500-24-2f	353	18552	19.9447	19.8893	55.4	41.558	0.800
Fe-Eo-3500-24-3f	354	18552	19.9449	19.9060	38.9	41.579	0.561
Fe-Eo-3500-24-2p	356	18552	20.4940	20.4578	36.2	22.496	0.965
Fe-Eo-3500-24-3p	357	18552	20.5446	20.5144	30.2	21.919	0.826
Fe-Atm-3500-24-2	359	18552	20.6528	20.6531	-0.3	41.747	-0.004
Fe-Atm-3500-24-3	360	18552	20.6299	20.6294	0.5	41.649	0.007

Source: WIPP-FePb-3 Supplemental Binder C (ERMS 546084)

Table A- 2 Summary of Lead Coupon Corrosion Rate Data

Test ID	Coupon	Duration (hours)	Initial Wt (g)	Final Wt (g) (Calculated)	Weight Loss (mg)	Surface Area (cm ²)	Corrosion Rate (µm/yr)
Pb-G-0000-6-2f	L083	5304	34.9565	34.9425	14.0	43.101	0.473
Pb-G-0000-6-3f	L084	5304	35.0169	35.0062	10.7	42.560	0.366
Pb-G-0000-6-2p	L086	5304	34.9627	34.9504	12.3	23.784	0.753
Pb-G-0000-6-3p	L087	5304	34.7895	34.7807	8.8	22.407	0.572
Pb-Go-0000-6-1f	L089	5304	35.9965	35.9886	7.9	42.720	0.269
Pb-Go-0000-6-2f	L090	5304	35.2017	35.1957	6.0	42.920	0.204
Pb-Go-0000-6-1p	L091	5304	35.4321	35.4251	7.0	25.151	0.405
Pb-Go-0000-6-3p	L093	5304	35.5347	35.5272	7.5	23.720	0.461
Pb-E-0000-6-1f	L094	5304	35.4331	35.4250	8.1	42.969	0.275
Pb-E-0000-6-2f	L095	5304	36.0654	36.0600	5.4	42.895	0.183
Pb-E-0000-6-1p	L097	5304	35.8988	35.8895	9.3	25.225	0.537
Pb-E-0000-6-2p	L098	5304	34.4660	34.4546	11.4	25.287	0.657
Pb-Eo-0000-6-1f	L100	5304	35.4418	35.4369	4.9	42.574	0.168
Pb-Eo-0000-6-2f	L101	5304	35.3272	35.3223	4.9	42.586	0.168
Pb-Eo-0000-6-1p	L103	5304	35.6308	35.6220	8.8	25.949	0.494
Pb-Eo-0000-6-2p	L104	5304	35.1904	35.1825	7.9	25.703	0.448
Pb-Atm-0000-6-1	L106	5304	35.9058	35.9051	0.7	42.637	0.024
Pb-Atm-0000-6-2	L107	5304	35.4546	35.4517	2.9	43.091	0.098
Pb-G-0350-6-1f	L109	5808	34.8781	34.8744	3.7	42.860	0.115
Pb-G-0350-6-2f	L110	5808	35.4684	35.4633	5.1	42.759	0.159
Pb-G-0350-6-1p	L112	5808	35.1391	35.1362	2.9	24.120	0.160
Pb-G-0350-6-2p	L113	5808	34.6572	34.6431	14.1	23.093	0.812
Pb-Go-0350-6-1f	L115	5808	35.0723	35.0626	9.7	42.960	0.300
Pb-Go-0350-6-2f	L116	5808	35.1860	35.1974	-11.4	42.602	-0.356
Pb-Go-0350-6-1p	L118	5808	35.5343	35.5356	-1.3	26.318	-0.066
Pb-Go-0350-6-2p	L119	5808	35.6150	35.6071	7.9	24.690	0.426
Pb-E-0350-6-1f	L121	5808	34.6720	34.6668	5.2	42.451	0.163
Pb-E-0350-6-2f	L122	5808	35.3743	35.3677	6.6	42.709	0.206
Pb-E-0350-6-1p	L124	5808	35.3672	35.3638	3.4	27.340	0.165
Pb-E-0350-6-2p	L125	5808	35.8618	35.8569	4.9	26.866	0.243
Pb-Eo-0350-6-1f	L127	5808	34.6510	34.6404	10.6	42.616	0.331
Pb-Eo-0350-6-2f	L128	5808	34.8518	34.8429	8.9	43.014	0.275
Pb-Eo-0350-6-1p	L130	5808	35.4064	35.3985	7.9	25.160	0.418
Pb-Eo-0350-6-2p	L131	5808	35.0594	35.0541	5.3	24.301	0.290
Pb-Atm-0350-6-1	L133	5808	35.1639	35.1650	-1.1	42.745	-0.034
Pb-Atm-0350-6-2	L134	5808	35.3418	35.3435	-1.7	42.864	-0.053
Pb-G-1500-6-1f	L299	5064	35.1086	35.1001	8.5	41.986	0.309
Pb-G-1500-6-2f	L300	5064	36.0213	36.0137	7.6	42.156	0.275
Pb-G-1500-6-1p	L302	5064	35.9088	35.8793	29.5	22.383	2.010
Pb-G-1500-6-2p	L303	5064	35.5716	35.5546	17.0	24.413	1.062
Pb-Go-1500-6-1f	L305	5064	34.6158	34.6036	12.2	42.651	0.436
Pb-Go-1500-6-2f	L306	5064	34.8760	34.8621	13.9	42.390	0.500
Pb-Go-1500-6-1p	L308	5064	35.0408	35.0221	18.7	21.148	1.349
Pb-Go-1500-6-2p	L309	5064	34.8474	34.8274	20.0	20.147	1.514

Test ID	Coupon	Duration (hours)	Initial Wt (g)	Final Wt (g) (Calculated)	Weight Loss (mg)	Surface Area (cm ²)	Corrosion Rate (µm/yr)
Pb-E-1500-6-1f	L311	5064	36.0171	36.0132	3.9	42.671	0.139
Pb-E-1500-6-2f	L312	5064	34.1353	34.1305	4.8	42.462	0.172
Pb-E-1500-6-1p	L314	5064	34.8270	34.8128	14.2	24.654	0.879
Pb-E-1500-6-2p	L315	5064	35.7921	35.7813	10.8	24.013	0.686
Pb-Eo-1500-6-1f	L317	5064	35.8858	35.8788	7.0	42.653	0.250
Pb-Eo-1500-6-2f	L318	5064	34.8114	34.8040	7.4	42.866	0.263
Pb-Eo-1500-6-1p	L320	5064	35.3177	35.3072	10.5	25.154	0.637
Pb-Eo-1500-6-2p	L321	5064	34.6691	34.6548	14.3	24.534	0.889
Pb-Atm-1500-6-1	L323	5064	35.0368	35.0336	3.2	42.222	0.116
Pb-Atm-1500-6-2	L324	5064	35.1052	35.1000	5.2	42.888	0.185
Pb-G-3500-6-1f	L413	4968	34.6030	34.5922	10.8	42.507	0.395
Pb-G-3500-6-2f	L414	4968	34.2356	34.2262	9.4	42.671	0.343
Pb-G-3500-6-2p	L417	4968	35.1097	35.0965	13.2	22.987	0.893
Pb-G-3500-6-3p	L418	4968	34.9317	34.9201	11.6	23.048	0.783
Pb-Go-3500-6-1f	L419	4968	34.9312	34.9194	11.8	42.575	0.431
Pb-Go-3500-6-2f	L420	4968	34.1202	34.1119	8.3	42.344	0.305
Pb-Go-3500-6-1p	L422	4968	34.7956	34.7837	11.9	26.414	0.701
Pb-Go-3500-6-2p	L423	4968	35.1465	35.1292	17.3	25.304	1.063
Pb-E-3500-6-1f	L425	4968	34.3943	34.3891	5.2	41.956	0.193
Pb-E-3500-6-2f	L426	4968	34.1568	34.1452	11.6	42.583	0.424
Pb-E-3500-6-1p	L428	4968	35.1248	35.1098	15.0	22.821	1.022
Pb-E-3500-6-2p	L429	4968	34.6425	34.6245	18.0	21.888	1.279
Pb-Eo-3500-6-1f	L431	4968	34.7844	34.7754	9.0	42.324	0.331
Pb-Eo-3500-6-2f	L432	4968	34.7211	34.7132	7.9	42.474	0.289
Pb-Eo-3500-6-1p	L434	4968	34.8573	34.8476	9.7	25.321	0.596
Pb-Eo-3500-6-2p	L435	4968	35.1251	35.1154	9.7	24.396	0.618
Pb-Atm-3500-6-2	L453	4968	34.9586	34.9565	2.1	42.307	0.077
Pb-Atm-3500-6-3	L454	4968	34.7891	34.7879	1.2	42.427	0.044
Pb-G-0000-12-1f	L055	8904	35.3378	35.3270	10.8	42.547	0.220
Pb-G-0000-12-2f	L056	8904	34.0622	34.0532	9.0	42.959	0.182
Pb-G-0000-12-1p	L058	8904	36.0145	36.0028	11.7	22.993	0.441
Pb-G-0000-12-2p	L059	8904	34.7627	34.7490	13.7	23.051	0.516
Pb-Go-0000-12-1f	L061	8904	34.1481	34.1307	17.4	42.874	0.352
Pb-Go-0000-12-2f	L062	8904	34.1944	34.1858	8.6	42.495	0.176
Pb-Go-0000-12-1p	L064	8904	35.8906	35.8766	14.0	21.264	0.571
Pb-Go-0000-12-2p	L065	8904	35.3656	35.3524	13.2	21.002	0.545
Pb-E-0000-12-2f	L068	8904	36.0855	36.0766	8.9	42.736	0.181
Pb-E-0000-12-3f	L069	8904	36.1265	36.1220	4.5	42.674	0.091
Pb-E-0000-12-2p	L071	8904	33.9754	33.9621	13.3	25.314	0.456
Pb-E-0000-12-3p	L072	8904	33.9791	33.9665	12.6	23.223	0.471
Pb-Eo-0000-12-2f	L074	8904	35.3804	35.3757	4.7	43.261	0.094
Pb-Eo-0000-12-3f	L075	8904	35.1943	35.1833	11.0	42.824	0.223
Pb-Eo-0000-12-1p	L076	8904	35.3162	35.3046	11.6	23.096	0.436
Pb-Eo-0000-12-2p	L077	8904	34.6883	34.6731	15.2	23.368	0.564
Pb-Atm-0000-12-1	L079	8904	34.5752	34.5705	4.7	43.180	0.094

Test ID	Coupon	Duration (hours)	Initial Wt (g)	Final Wt (g) (Calculated)	Weight Loss (mg)	Surface Area (cm ²)	Corrosion Rate (µm/yr)
Pb-Atm-0000-12-2	L080	8904	34.9096	34.9033	6.3	43.252	0.126
Pb-G-0350-12-1f	L190	8760	35.3755	35.3648	10.7	42.232	0.223
Pb-G-0350-12-2f	L191	8760	36.1066	36.0964	10.2	42.177	0.213
Pb-G-0350-12-2p	L194	8760	34.6025	34.6029	-0.4	24.084	-0.015
Pb-G-0350-12-3p	L195	8760	34.6846	34.6793	5.3	24.066	0.194
Pb-Go-0350-12-1f	L196	8760	35.2779	35.2688	9.1	42.130	0.190
Pb-Go-0350-12-3f	L198	8760	36.1804	36.1648	15.6	42.078	0.327
Pb-Go-0350-12-1p	L199	8760	35.2663	35.2696	-3.3	24.401	-0.119
Pb-Go-0350-12-2p	L200	8760	35.9647	35.9593	5.4	23.795	0.200
Pb-E-0350-12-2f	L203	8760	35.3566	35.3824	-25.8	41.989	-0.542
Pb-E-0350-12-3f	L204	8760	35.3174	35.3161	1.3	42.056	0.027
Pb-E-0350-12-1p	L205	8760	34.5903	34.5897	0.6	25.602	0.021
Pb-E-0350-12-3p	L207	8760	36.2173	36.2095	7.8	25.223	0.273
Pb-Eo-0350-12-2f	L209	8760	35.4896	35.4886	1.0	42.113	0.021
Pb-Eo-0350-12-3f	L210	8760	35.1431	35.1329	10.2	42.032	0.214
Pb-Eo-0350-12-1p	L211	8760	35.2497	35.2378	11.9	30.914	0.339
Pb-Eo-0350-12-2p	L212	8760	35.1299	35.1283	1.6	30.709	0.046
Pb-Atm-0350-12-1	L214	8760	35.1582	35.1602	-2.0	42.012	-0.042
Pb-Atm-0350-12-2	L215	8760	35.2606	35.2560	4.6	41.992	0.097
Pb-G-1500-12-2f	L272	9000	34.5033	34.4886	14.7	42.492	0.297
Pb-G-1500-12-3f	L273	9000	34.8008	34.7912	9.6	42.115	0.196
Pb-G-1500-12-2p	L275	9000	35.3713	35.3528	18.5	23.794	0.667
Pb-G-1500-12-3p	L276	9000	34.8719	34.8532	18.7	23.649	0.679
Pb-Go-1500-12-1f	L277	9000	34.9428	34.9349	7.9	42.389	0.160
Pb-Go-1500-12-2f	L278	9000	34.7336	34.7241	9.5	42.102	0.194
Pb-Go-1500-12-1p	L280	9000	35.0697	35.0544	15.3	27.327	0.481
Pb-Go-1500-12-2p	L281	9000	35.8230	35.8051	17.9	26.337	0.583
Pb-E-1500-12-1f	L283	9000	36.0889	36.0817	7.2	41.956	0.147
Pb-E-1500-12-3f	L285	9000	36.1523	36.1476	4.7	42.274	0.095
Pb-E-1500-12-1p	L286	9000	34.9871	34.9682	18.9	23.734	0.684
Pb-E-1500-12-2p	L287	9000	34.7513	34.7326	18.7	26.655	0.602
Pb-Eo-1500-12-2f	L290	9000	35.8010	35.7934	7.6	42.152	0.155
Pb-Eo-1500-12-3f	L291	9000	35.8531	35.8446	8.5	42.462	0.172
Pb-Eo-1500-12-1p	L292	9000	35.8814	35.8667	14.7	23.900	0.528
Pb-Eo-1500-12-2p	L293	9000	35.8772	35.8620	15.2	23.329	0.559
Pb-Atm-1500-12-1	L295	9000	36.1501	36.1463	3.8	42.390	0.077
Pb-Atm-1500-12-2	L297	9000	34.9107	34.9035	7.2	42.364	0.146
Pb-G-3500-12-1f	L386	9192	34.9965	34.9893	7.2	42.582	0.142
Pb-G-3500-12-2f	L387	9192	36.1403	36.1293	11.0	42.538	0.217
Pb-G-3500-12-1p	L389	9192	34.7017	34.6910	10.7	25.442	0.353
Pb-G-3500-12-2p	L390	9192	34.6293	34.6156	13.7	24.427	0.471
Pb-Go-3500-12-1f	L392	9192	34.9198	34.9082	11.6	42.005	0.232
Pb-Go-3500-12-2f	L393	9192	34.3856	34.3793	6.3	41.714	0.127
Pb-Go-3500-12-1p	L395	9192	35.0050	35.0004	4.6	23.862	0.162
Pb-Go-3500-12-2p	L396	9192	34.1048	34.0989	5.9	22.224	0.223

Test ID	Coupon	Duration (hours)	Initial Wt (g)	Final Wt (g) (Calculated)	Weight Loss (mg)	Surface Area (cm ²)	Corrosion Rate (µm/yr)
Pb-E-3500-12-1f	L398	9192	34.6465	34.6452	1.3	41.904	0.026
Pb-E-3500-12-2f	L399	9192	34.4017	34.4032	-1.5	41.947	-0.030
Pb-E-3500-12-1p	L401	9192	34.0783	34.0683	10.0	25.079	0.335
Pb-E-3500-12-2p	L402	9192	34.7546	34.7414	13.2	23.415	0.474
Pb-Eo-3500-12-1f	L404	9192	34.6299	34.6217	8.2	42.373	0.163
Pb-Eo-3500-12-2f	L405	9192	33.8274	33.8195	7.9	42.513	0.156
Pb-Eo-3500-12-1p	L407	9192	33.8222	33.8115	10.7	25.065	0.359
Pb-Eo-3500-12-2p	L408	9192	35.2047	35.1998	4.9	25.497	0.162
Pb-Atm-3500-12-1	L410	9192	34.1198	34.1149	4.9	42.421	0.097
Pb-Atm-3500-12-2	L411	9192	34.8854	34.8814	4.0	42.601	0.079
Pb-G-0000-18-2f	L029	13368	34.3063	34.3048	1.5	41.978	0.021
Pb-G-0000-18-3f	L030	13368	34.3276	34.3262	1.4	42.559	0.019
Pb-G-0000-18-2p	L032	13368	34.4391	34.4314	7.7	23.356	0.191
Pb-G-0000-18-3p	L033	13368	34.5575	34.5489	8.6	25.387	0.196
Pb-Go-0000-18-2f	L035	13368	35.1404	35.1329	7.5	42.650	0.102
Pb-Go-0000-18-3f	L036	13368	34.3672	34.3608	6.4	42.509	0.087
Pb-Go-0000-18-2p	L038	13368	33.9740	33.9713	2.7	25.538	0.061
Pb-Go-0000-18-3p	L039	13368	35.6926	35.6815	11.1	26.607	0.241
Pb-E-0000-18-2f	L041	13368	34.0598	34.0580	1.8	41.752	0.025
Pb-E-0000-18-3f	L042	13368	34.3987	34.3919	6.8	41.863	0.094
Pb-E-0000-18-2p	L044	13368	34.7290	34.7215	7.5	19.442	0.223
Pb-E-0000-18-3p	L045	13368	34.6101	34.5955	14.6	24.422	0.345
Pb-Eo-0000-18-2f	L047	13368	34.5793	34.5784	0.9	41.898	0.012
Pb-Eo-0000-18-3f	L048	13368	33.9877	33.9883	-0.6	41.794	-0.008
Pb-Eo-0000-18-2p	L050	13368	35.5817	35.5717	10.0	26.013	0.222
Pb-Eo-0000-18-3p	L051	13368	35.1003	35.0946	5.7	26.409	0.125
Pb-Atm-0000-18-2	L053	13368	34.9513	34.9512	0.1	43.094	0.001
Pb-Atm-0000-18-3	L054	13368	35.1549	35.1531	1.8	43.246	0.024
Pb-G-0350-18-2f	L164	13272	34.0606	34.0544	6.2	42.420	0.085
Pb-G-0350-18-3f	L165	13272	35.3544	35.3452	9.2	42.944	0.125
Pb-G-0350-18-2p	L167	13272	34.4808	34.4740	6.8	22.601	0.175
Pb-G-0350-18-3p	L168	13272	35.0329	35.0258	7.1	22.761	0.182
Pb-Go-0350-18-2f	L170	13272	35.2164	35.2071	9.3	42.914	0.126
Pb-Go-0350-18-3f	L171	13272	35.8826	35.8751	7.5	42.585	0.103
Pb-Go-0350-18-2p	L173	13272	35.9921	35.9869	5.2	24.127	0.125
Pb-Go-0350-18-3p	L174	13272	34.5597	34.5497	10.0	24.606	0.237
Pb-E-0350-18-2f	L176	13272	35.8624	35.8550	7.4	42.359	0.102
Pb-E-0350-18-3f	L177	13272	35.9128	35.9059	6.9	42.341	0.095
Pb-E-0350-18-2p	L179	13272	36.0121	36.0039	8.2	24.729	0.193
Pb-E-0350-18-3p	L180	13272	35.9762	35.9710	5.2	22.169	0.137
Pb-Eo-0350-18-2f	L182	13272	35.7734	35.7657	7.7	42.292	0.106
Pb-Eo-0350-18-3f	L183	13272	34.5553	34.5514	3.9	42.319	0.054
Pb-Eo-0350-18-2p	L185	13272	36.1124	36.1065	5.9	24.561	0.140
Pb-Eo-0350-18-3p	L186	13272	36.0568	36.0477	9.1	23.551	0.225
Pb-Atm-0350-18-2	L188	13272	34.7444	34.7409	3.5	42.037	0.048

Test ID	Coupon	Duration (hours)	Initial Wt (g)	Final Wt (g) (Calculated)	Weight Loss (mg)	Surface Area (cm ²)	Corrosion Rate (µm/yr)
Pb-Atm-0350-18-3	L189	13272	34.8288	34.8257	3.1	42.073	0.043
Pb-G-1500-18-2f	L245	13608	34.8306	34.8215	9.1	42.998	0.120
Pb-G-1500-18-3f	L246	13608	35.3314	35.3214	10.0	42.786	0.133
Pb-G-1500-18-2p	L248	13608	35.4782	35.4695	8.7	25.951	0.190
Pb-G-1500-18-3p	L249	13608	34.7978	34.7837	14.1	24.407	0.328
Pb-Go-1500-18-2f	L251	13608	34.9622	34.9421	20.1	42.991	0.265
Pb-Go-1500-18-3f	L252	13608	35.5246	35.5164	8.2	42.336	0.110
Pb-Go-1500-18-2p	L254	13608	35.1169	35.1044	12.5	26.783	0.265
Pb-Go-1500-18-3p	L255	13608	35.1302	35.1197	10.5	25.132	0.237
Pb-E-1500-18-2f	L257	13608	34.7452	34.7384	6.8	42.154	0.092
Pb-E-1500-18-3f	L258	13608	35.4430	35.4409	2.1	42.555	0.028
Pb-E-1500-18-2p	L260	13608	34.1285	34.1271	1.4	23.301	0.034
Pb-E-1500-18-3p	L261	13608	34.6729	34.6743	-1.4	23.252	-0.034
Pb-Eo-1500-18-2f	L263	13608	34.8119	34.8093	2.6	42.523	0.035
Pb-Eo-1500-18-3f	L264	13608	34.6367	34.6357	1.0	42.867	0.013
Pb-Eo-1500-18-2p	L266	13608	34.8324	34.8235	8.9	24.336	0.208
Pb-Eo-1500-18-3p	L267	13608	34.7187	34.7081	10.6	25.180	0.239
Pb-Atm-1500-18-2	L269	13608	35.1766	35.1775	-0.9	42.211	-0.012
Pb-Atm-1500-18-3	L270	13608	34.5613	34.5577	3.6	42.366	0.048
Pb-G-3500-18-2f	L359	13704	34.4345	34.4156	18.9	42.995	0.248
Pb-G-3500-18-3f	L360	13704	35.1906	35.1736	17.0	42.973	0.223
Pb-G-3500-18-2p	L362	13704	35.7358	35.7282	7.6	24.618	0.174
Pb-G-3500-18-3p	L363	13704	35.4985	35.4888	9.7	26.172	0.209
Pb-Go-3500-18-2f	L365	13704	35.1688	35.1560	12.8	42.601	0.169
Pb-Go-3500-18-3f	L366	13704	35.9119	35.8990	12.9	42.320	0.172
Pb-Go-3500-18-2p	L368	13704	35.3528	35.3521	0.7	25.563	0.015
Pb-Go-3500-18-3p	L369	13704	35.3189	35.3054	13.5	26.007	0.293
Pb-E-3500-18-2f	L371	13704	35.1792	35.1814	-2.2	42.433	-0.029
Pb-E-3500-18-3f	L372	13704	35.0504	35.0562	-5.8	42.632	-0.077
Pb-E-3500-18-2p	L374	13704	35.3381	35.3465	-8.4	23.131	-0.205
Pb-E-3500-18-3p	L376	13704	34.6894	34.6962	-6.8	24.367	-0.157
Pb-Eo-3500-18-2f	L378	13704	35.2542	35.2497	4.5	42.450	0.060
Pb-Eo-3500-18-3f	L379	13704	36.0201	36.0188	1.3	42.417	0.017
Pb-Eo-3500-18-2p	L381	13704	34.6266	34.6288	-2.2	24.378	-0.051
Pb-Eo-3500-18-3p	L382	13704	36.0202	36.0203	-0.1	23.866	-0.002
Pb-Atm-3500-18-2	L384	13704	35.3341	35.3261	8.0	42.617	0.106
Pb-Atm-3500-18-3	L385	13704	36.0778	36.0753	2.5	42.508	0.033
Pb-G-0000-24-2f	L002	18528	35.5556	35.5431	12.5	42.915	0.121
Pb-G-0000-24-3f	L003	18528	35.6341	35.6168	17.3	42.780	0.169
Pb-G-0000-24-2p	L005	18528	35.1444	35.1352	9.2	24.421	0.157
Pb-G-0000-24-3p	L006	18528	35.3700	35.3623	7.7	19.716	0.163
Pb-Go-0000-24-2f	L008	18528	35.3503	35.3417	8.6	42.875	0.084
Pb-Go-0000-24-3f	L009	18528	35.2176	35.2103	7.3	43.017	0.071
Pb-Go-0000-24-2p	L011	18528	35.2259	35.2213	4.6	25.280	0.076
Pb-Go-0000-24-3p	L012	18528	35.9487	35.9541	-5.4	24.119	-0.093

Test ID	Coupon	Duration (hours)	Initial Wt (g)	Final Wt (g) (Calculated)	Weight Loss (mg)	Surface Area (cm ²)	Corrosion Rate (µm/yr)
Pb-E-0000-24-2f	L014	18528	35.1179	35.1134	4.5	42.415	0.044
Pb-E-0000-24-3f	L015	18528	35.0627	35.0565	6.2	42.534	0.061
Pb-E-0000-24-2p	L017	18528	35.3128	35.3050	7.8	23.570	0.138
Pb-E-0000-24-3p	L018	18528	34.7897	34.7869	2.8	25.444	0.046
Pb-Eo-0000-24-2f	L020	18528	35.7989	35.8024	-3.5	43.034	-0.034
Pb-Eo-0000-24-3f	L021	18528	35.0101	35.0111	-1.0	42.388	-0.010
Pb-Eo-0000-24-2p	L023	18528	35.5732	35.5681	5.1	28.616	0.074
Pb-Eo-0000-24-3p	L024	18528	34.7456	34.7417	3.9	26.205	0.062
Pb-Atm-0000-24-2	L026	18528	34.7043	34.7037	0.6	41.718	0.006
Pb-Atm-0000-24-3	L027	18528	34.5269	34.5281	-1.2	41.633	-0.012
Pb-G-0350-24-2f	L137	18288	35.4022	35.3882	14.0	42.615	0.139
Pb-G-0350-24-3f	L138	18288	35.8065	35.7882	18.3	42.626	0.181
Pb-G-0350-24-2p	L140	18288	35.1586	35.1452	13.4	27.529	0.206
Pb-G-0350-24-3p	L141	18288	36.0541	36.0442	9.9	22.499	0.186
Pb-Go-0350-24-2f	L143	18288	35.8544	35.8433	11.1	42.558	0.110
Pb-Go-0350-24-3f	L144	18288	35.2684	35.2659	2.5	43.021	0.025
Pb-Go-0350-24-2p	L146	18288	35.8863	35.8775	8.8	26.833	0.139
Pb-Go-0350-24-3p	L147	18288	35.9994	35.9907	8.7	27.495	0.134
Pb-E-0350-24-2f	L149	18288	34.5729	34.5637	9.2	42.355	0.092
Pb-E-0350-24-3f	L150	18288	34.5257	34.5143	11.4	42.671	0.113
Pb-E-0350-24-2p	L152	18288	35.8550	35.8436	11.4	27.162	0.177
Pb-E-0350-24-3p	L153	18288	35.8579	35.8543	3.6	26.465	0.057
Pb-Eo-0350-24-2f	L155	18288	36.0256	36.0172	8.4	42.521	0.083
Pb-Eo-0350-24-3f	L156	18288	35.8608	35.8585	2.3	42.476	0.023
Pb-Eo-0350-24-2p	L158	18288	35.9581	35.9456	12.5	29.356	0.180
Pb-Eo-0350-24-3p	L159	18288	34.7519	34.7441	7.8	30.568	0.108
Pb-Atm-0350-24-2	L161	18288	34.7789	34.7763	2.6	42.829	0.026
Pb-Atm-0350-24-3	L162	18288	35.9799	35.9808	-0.9	42.694	-0.009
Pb-G-1500-24-2f	L218	18840	34.4518	34.4385	13.3	42.269	0.129
Pb-G-1500-24-3f	L219	18840	36.1254	36.1125	12.9	42.357	0.125
Pb-G-1500-24-2p	L221	18840	34.5919	34.5866	5.3	27.009	0.080
Pb-G-1500-24-3p	L222	18840	34.2593	34.2597	-0.4	27.526	-0.006
Pb-Go-1500-24-2f	L224	18840	35.6093	35.5980	11.3	42.405	0.109
Pb-Go-1500-24-3f	L225	18840	35.5335	35.5240	9.5	42.230	0.092
Pb-Go-1500-24-2p	L227	18840	35.1164	35.1079	8.5	26.263	0.133
Pb-Go-1500-24-3p	L228	18840	35.8951	35.8845	10.6	27.289	0.159
Pb-E-1500-24-2f	L230	18840	35.5537	35.5495	4.2	42.447	0.041
Pb-E-1500-24-3f	L231	18840	35.1384	35.1230	15.4	42.788	0.148
Pb-E-1500-24-2p	L233	18840	34.5084	34.5026	5.8	25.386	0.094
Pb-E-1500-24-3p	L234	18840	34.5747	34.5624	12.3	24.221	0.208
Pb-Eo-1500-24-2f	L236	18840	36.2002	36.1905	9.7	42.529	0.094
Pb-Eo-1500-24-3f	L237	18840	35.8591	35.8532	5.9	42.077	0.057
Pb-Eo-1500-24-2p	L239	18840	36.0527	36.0426	10.1	25.452	0.163
Pb-Eo-1500-24-3p	L240	18840	35.9020	35.8917	10.3	25.230	0.167
Pb-Atm-1500-24-2	L242	18840	34.4960	34.4914	4.6	42.819	0.044

Test ID	Coupon	Duration (hours)	Initial Wt (g)	Final Wt (g) (Calculated)	Weight Loss (mg)	Surface Area (cm ²)	Corrosion Rate (µm/yr)
Pb-Atm-1500-24-3	L243	18840	36.0800	36.0736	6.4	42.698	0.061
Pb-G-3500-24-2f	L327	18552	35.5565	35.5452	11.3	42.644	0.110
Pb-G-3500-24-3f	L328	18552	35.0274	35.0155	11.9	42.119	0.118
Pb-G-3500-24-2p	L330	18552	35.4251	35.4078	17.3	25.005	0.288
Pb-G-3500-24-3p	L331	18552	35.3204	35.3031	17.3	24.143	0.298
Pb-Go-3500-24-2f	L333	18552	35.9784	35.9663	12.1	42.425	0.119
Pb-Go-3500-24-3f	L334	18552	36.1270	36.1143	12.7	42.312	0.125
Pb-Go-3500-24-2p	L337	18552	35.0805	35.0598	20.7	26.375	0.327
Pb-Go-3500-24-3p	L339	18552	35.0693	35.0423	27.0	24.763	0.454
Pb-E-3500-24-2f	L341	18552	35.8415	35.8398	1.7	42.932	0.016
Pb-E-3500-24-3f	L342	18552	34.6500	34.6474	2.6	42.855	0.025
Pb-E-3500-24-2p	L344	18552	34.4406	34.4327	7.9	25.264	0.130
Pb-E-3500-24-3p	L345	18552	34.9862	34.9817	4.5	24.471	0.077
Pb-Eo-3500-24-2f	L347	18552	34.7670	34.7620	5.0	43.027	0.048
Pb-Eo-3500-24-3f	L348	18552	35.9570	35.9535	3.5	42.970	0.034
Pb-Eo-3500-24-2p	L350	18552	34.7657	34.7591	6.6	24.972	0.110
Pb-Eo-3500-24-3p	L353	18552	35.7837	35.7739	9.8	26.539	0.154
Pb-Atm-3500-24-2	L356	18552	35.3392	35.3315	7.7	42.970	0.075
Pb-Atm-3500-24-3	L357	18552	35.4526	35.4492	3.4	42.935	0.033

Source: WIPP-FePb-3 Supplemental Binder C (ERMS 546084)